Mineralogy and petrography of primary copper mineralization from Moonta Mines

Thesis submitted in accordance with the requirements of the University of Adelaide for an Honours Degree in Geology

Dale Cameron

October 2014

MINERALOGY AND PETROGRAPHY OF PRIMARY COPPER MINERALIZATION FROM MOONTA MINES: A RE-INVESTIGATION OF MCBRIAR'S 1962 THESIS SAMPLE SUITE

MINERALOGY AND PETROGRAPHY: MOONTA-WALLAROO

ABSTRACT

Samples of massive bornite- and chalcopyrite ore from the Moonta and Wallaroo Mines, originally collected by Erica Maud McBriar for her M.Sc. thesis in 1962, have been investigated to determine mineralogical and petrographic relationships between co-existing minerals. Much is known about the mining history of Moonta-Wallaroo but few previous studies have attempted to characterise the mineralization itself and compare it with that present elsewhere. Results show that massive copper ores from the Moonta and Wallaroo Mines share a number of mineralogical and textural similarities with other IOCG systems in the Olympic Cu-Au Province. Other mineralogical features, such as the abundant pyrrhotite, appear to be a reflection of unusually reduced conditions, although late, superposed hematite infers a shift towards oxidized conditions in the final stages of mineralization.

The replacement of bornite by chalcopyrite and of chalcopyrite by bornite, even in the same sample is suggestive of multiple episodes of ore crystallization, possibly during a single protracted event. The observations do not contradict established models of ore genesis in which the Moonta orebodies are the products of structurally-controlled IOCG-style mineralization. Ore-forming fluids were likely derived from ~1.6 Ga Hiltaba Suite intrusives and driven along shear zones. The study, based around polished sections prepared from precious sample material collected more than 50 years ago contribute to a genetic model that takes account of the diversity of mineralization styles, which can assist with ongoing exploration in the Moonta-Wallaroo area.

KEYWORDS

IOCG, Moonta-Wallaroo, Petrology, Sulphide Mineralization, Alteration.

TABLE OF CONTENTS

LIST OF FIGURES AND TABLES

Figure 13: *Sample 162/11 – Chalcopyrite (Bell Metal): (a) Image shows the general distribution of the chalcopyrite with gangue grains and tiny pyrite inclusions, (b) Bell Metal chalcopyrite is effected by anhedral pyrite inhabitants, (c) Bell Metal chalcopyrite contains rare inclusions of apatite and what is interpreted as Malayaite (An Sn bearing Hydrothermal alteration of cassiterite-quartz assemblage and Sn-bearing skarns. Structurally related to titanite.),(d) Tiny rare inclusion of apatite within a 30um pyrite grain within the bell-metal chalcopyrite*

Figure 14: *Sample 162/53 – Sphalerite Sulphide: (a) Sphalerite grains are massive and euhedral, grains extend up to 3mm in size, (b) The matrix is made up of some sort of aluminosilicate, darker areas are presumed to be calcite as they are high in calcium, where they grey gangue mineral is calcium depleted. The matrix is host to small phenocrysts of pyrite and Sphalerite grains, (c) Chalcopyrite is common throughout the sample as anhedral grains that plays host to pyrite inclusions, (d) Where the Sphalerite grains meet the matrix there is a defined border of calcium enriched aluminosilicate that also hosts to small chalcopyrite and pyrite grains.*

Figure 15: *Sample 162/10: (a-d) Reflected light photomicrographs showing exsolution of tiny bornite granules within chalcopyrite. The excreted bornite tends to have a linear distribution, following crystallographic planes in the host mineral. (e and f) Relationship between hematite and chalcopyrite suggestive of later overgrowth.*

Figure 16: Sample 162/53 (sphalerite): Two distinct pyrite morphologies co-exist. There are smaller Euhedral grains (Eu) that often occur as inclusions within chalcopyrite, and anhedral grains (An) that are observed outside of the chalcopyrite within gangue quartz.

Figure 17: (a) *Sample 162/104 – Pyrrhotite: Fractured Pyrrhotite hosts many inclusions, majorly being hornblende and apatite, (b) Sample 162/104 – Pyrrhotite: Elongate stringer grains containing Ma.*

Figure 18: *Sample 162/49 – Cobaltite Sulphide: (a) Sample is dominated by abundant Pyrite with a rare native Bismuth granule no bigger than 50µm, gangue matrix is composed of Calcite and other aluminosilicates (b) Fractured areas within the Pyrite can sometimes contain chalcopyrite mineralization along with the Calcite gangue, (c) Cobaltite grains are scarce but large in size (1-2mm), the grains are euhedral and heavily fractured. Pyrite grains are also euhedral and similar in size, however can range from 20µm-1.5mm, (d) Within the fractures of the Cobaltite, quartz mineral growth has occurred along with the odd chalcopyrite granule.*

Figure 19: *Sample 162/66 – Covellite Sulphide: (a) The overall trend of the sample, covellite needles growing off the quartz gangue, (b) Deformed quartz is surrounded by covellite needle boundary with grain inclusions of Pyrite, (c) scarce amounts of tiny grains of rutile are present within the quartz, (d) Pyrite grains range up to 150µm in diameter within the covellite, (e) Rare orthoclase granules surrounded by covellite, (f) Titanite (or sphene), a calcium titanium nesosilicate is a rare inclusion within the deformed quartz groundmass.*

Figure 20*: Schematic diagram illustrating the main ingredients for IOCG-style mineralization in the Moonta area (sourced from Conor et al. 2010)*

Figure 21: *Sample 162/53 – Sphalerite Sulfide: A grain of Iron rich sulfides, Cu Zonation within the grain. The red line designates cu rich areas, those areas being determined as Chalcopyrite. The Cu Poor areas are pure Fe and S, with ratio of 1:2 favouring Sulfur, hence Pyrite. There are also small grains of Galena in the Sphalerite dominated sample.*

Figure 22: *Sample 162/59 – Bornite Sulfide: Uranium rich grains are within the voids of the bornite dominated groundmass. Hematite grains include inclusions of bornite and magnetite inclusions.*

Figure 23: Sample 162/106 – Moonta Hematite: (a) Iron Oxide Hematite needles are spontaneous and are *not in a lamellae form in amongst the aluminosilicate gangue, (b) Some Hematite needles contain inclusions from the aluminosilicate groundmass, (c) Some Hematite needles look like they have been eaten away from the inside, (d) Elongate quartz grains are spread amongst the hematite needles almost separating the gangue*

Figure 24: (a) *Sample 162/106 – Moonta Hematite: Big Parallel Fractures run throughout the whole sample, giving distinct growth restrains to the hematite needles, (b) Sample 162/106 – Moonta Hematite: Rare inclusion that is high in Y,Si and O, demonstrates a conchoidal grain distribution.*

Figure 25: *Sample 162/109 – Moonta Hematite: (a) Chalcopyrite and Hematite border is very sharp, showing no sharing of elements what so ever, (b) Euhedral Pyrite accessory grains within Chalcopyrite, quartz mineral growth through fracture zones, (c) Within the gangue, the majority is made of Albite Plagioclase with grains of apatite (>400um in size) with the odd inclusion of chalcopyrite, (d) Image shows the relationship between hematite and chalcopyrite*

Figure 26: (a) *Sample 162/110 – Ferberite: Ferberite grains are somewhat in a needle-type form. Ferberite consists roughly 75% of the sample. Some quartz inclusions are common throughout the voids, long elongate grains of chalcopyrite sulphides are common, (b) Sample 162/110 – Ferberite: The chalcopyrite inhabited elongate grains tend to grow in the fracture plains. Mineralization in the fracture plains also consists of a FeSiO.*

INTRODUCTION

The geological history of the Gawler Craton extends back to roughly 3400 Ma. The Gawler Craton (Figure 1) has experienced an extended history. Magmatic and orogenic events during the Neoarchean and Palaeoproterozoic include the Sleafordian (~2410 Ma) and Kimban (~1730 Ma) orogenies (Reid and Hand, 2012). A major magmatic event took place during the interval 1620-1570 Ma and involved intrusion of the Hiltaba Granite Series suite and eruption of coeval Gawler Range Volcanics (Conor et al., 2010). The 1620-1570 Ma magmatic event was also responsible for widespread mineralization and associated alteration, notably formation of numerous iron oxide-copper-gold (IOCG) deposits, including the giant Olympic Dam ore system (Resources as of June 2013: 1,408 Mt @ 1.08% Cu, 0.32kg/t U_3O_8, 0.34g/t Au and 2.07g/t Ag).

The mining history of South Australia however predates discovery of Olympic Dam in 1975. The Moonta and Wallaroo deposits, on the Yorke Peninsula, are also of IOCG-type and were first exploited as long ago as 1861 by Moonta Mining. These mines drove the early development of the South Australian economy and attracted a migrating population with the first deposits grading up to 30% Cu. They produced ores valued at more than $10 million (Zang et al., 2002). Although the Moonta-Wallaroo region continues to be an attractive exploration target, mining currently takes a back seat to agriculture within the area.

The Moonta-Wallaroo deposits are hosted within Palaeo- to Mesoproterozoic rocks of the Olympic Domain that extends along the eastern edge of the Gawler Craton, overlying Mesoarchaen to Palaeoproterozoic basement. They are partially overlain by thick Mesoproterozoic Gawler Range Volcanics (Conor et al., 2010). Neoproterozoic sediments of the Stuart Shelf unconformably overlie

these units. The local geology of the Moonta-Wallaroo district is defined by the major thermal event that took place approximately 1600-1575 Ma (Conor, 1996).

Mineralization in the Moonta-Wallaroo district mainly consists of Cu-Fe sulphide (chalcopyrite and bornite) orebodies, which are controlled locally by NE-trending shear zones. The main ore bodies are long, narrow veins or lodes, with pitches locally exceeding 80°. Their width never exceeds 3.5 metres. Copper grades are variable but tend to average around 4% in the ore lode zones. The lodes tend to be relatively shallow, (30 to 600 m from the surface; (Sokoloff, 1951). The lodes are hosted within a large feldspar porphyry body (Moonta Porphyry). This porphyry is felsic, consists mostly of plagioclase feldspar and albite, and was initially believed to belong to the Hiltaba Suite of intrusions (Jack, 1917). Today, the mines are inaccessible and ore samples are restricted to museum collections.

In the present mineralogical and petrographic study, optical and scanning electron microscopy are used to determine relationships among minerals within the Moonta-Wallaroo deposits. The study is based around 20 samples from a 1962 M.Sc. study by McBriar (McBriar 1962). These samples are all examples of massive sulphide from the main ore lodes. The aim of the study is to identify relationships, particularly among co-existing minerals, that can provide insights into the evolution of the deposits in the context of local geology, to identify any evidence pointing to secondary overprinting, and to compare results with those from other, better constrained IOCG systems in the Olympic Cu-Au province. This allows an appraisal of whether the Moonta and Wallaroo orebodies are unique within the overall perspective of IOCG mineralization because of their proximity to the Moonta Porphyry body.

GEOLOGICAL BACKGROUND

The Olympic Province, South Australia, is home to the World's largest known concentration of IOCG-style deposits (Figure 1). The Olympic Province is a an extensive metallogenic belt encompassing all of the IOCG mineralization in the Eastern Gawler Craton (Hayward and Skirrow, 2010). This province extends for over 700 km and hosts several economic IOCG systems including the World-class Olympic Dam (>9,000 Mt of ore; (Ehrig et al., 2012)), and Prominent Hill systems, as well as other more recent discoveries such as Carrapateena and Hillside that are currently under development. The Olympic Cu-Au Province also hosts numerous other prospects. These have been described by(Ferris et al., 2002), (Skirrow et al., 2002, Hayward and Skirrow, 2010). The tectonic history of the Gawler Craton has been documented in detail by Ferris *et al.* (2002), Hand *et al.* (2007) and Reid *et al.* (2008).

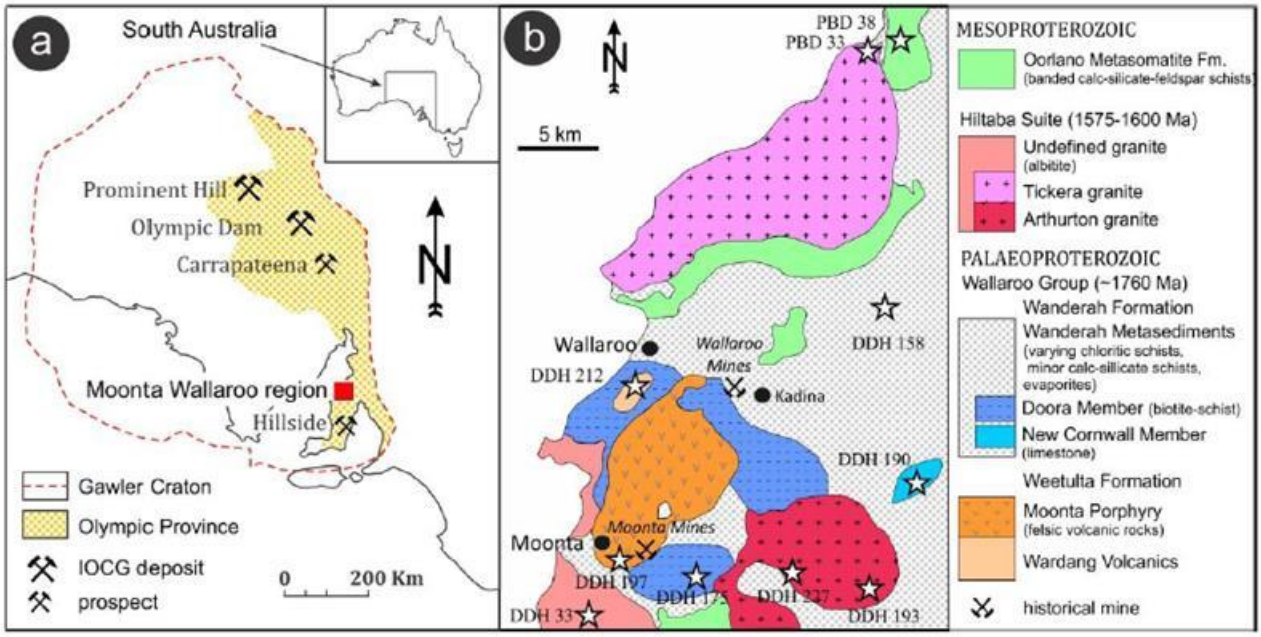

Figure 1: (a) Location Map of South Australia, detailing the location of the Moonta-Wallaroo region whilst also noting renowned deposits/prospects in the Olympic Province within the Gawler Craton. (b) Basement stratigraphy and locations of previous drill hole locations in the Moonta-Wallaroo Province (adapted from Conor et al. 2010; Forbes 2012).

The bedrock of the Olympic Cu-Au Province comprises Paleo- and Mesoproterozoic sediments, granites, volcanics and conglomerates (Conor et al., 2010, Hayward and Skirrow, 2010), underlain by Mesoarchean to Paleoproterozoic basement in the west (Ferris et al., 2002). Felsic plutonism (Hiltaba Suite), extrusive magmatism (Gawler Range Volcanics), and deposition of Cu-Au mineralization, is considered to immediately precede, the 1570-1540 Ma Kararan Orogeny (Hand et al., 2007, Reid et al., 2008). Whole-rock geochemical data show enrichment in Light Rare Earth Elements (LREE) within the felsic and mafic rock packages of the Olympic Province (Hand et al., 2007) as well as the orebodies. Conor *et al.* (2010) have considered the Moonta Porphyry within the Weetulta Formation of the ~1750 Ma Wallaroo Group. This interpretation derives from U-Pb SHRIMP zircon dating by Fanning *et al.* (2007) showing that felsic magmatism in the Wallaroo Group is 1772 ± 14 to 1735 ± 10 Ma in age (Figure 2).

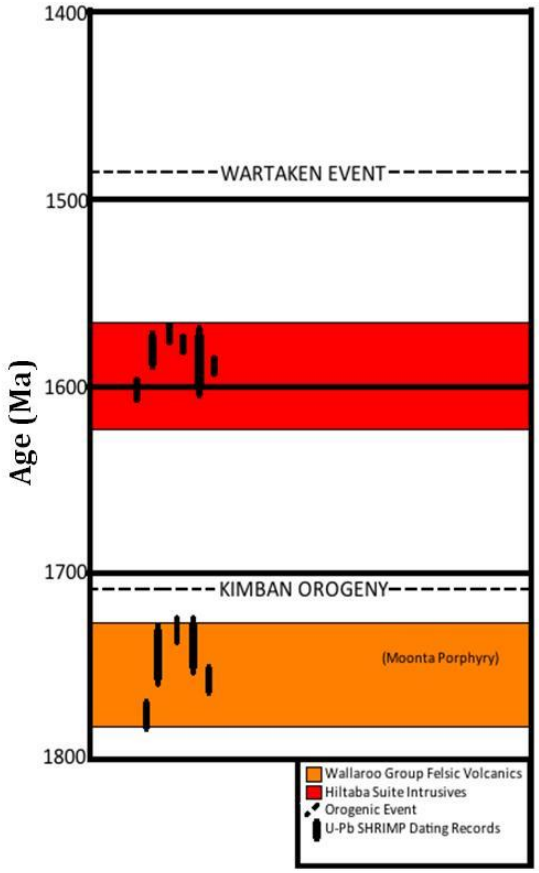

Figure 2: Schematic diagram showing the periods of magmatism and orogenic events within the Moonta-Wallaroo area

LOCAL GEOLOGY

Moonta Porphyry

The porphyry rock consists mostly of pale pink plagioclase feldspar phenocrysts that range up to 0.5mm. The phenocrysts are distributed through a very fine-grained, purplish-pink crystalline groundmass of porphyry, which contains dark green flakes of chlorite. The porphyry displays a glomeroporphyritic texture, i.e., the phenocrysts are commonly clustered within the matrix. The phenocrysts are either plagioclase feldspar or dark smoky quartz. The quartz is usually macroscopic in the form of veins with traces of chalcopyrite. Grain morphology is commonly rounded and shows slight secondary outgrowths and strain polarisation. Fine reddish needles of rutile cluster around the phenocrysts (Figure 3).

Figure 3*: Feldspar Porphyry- Normal Feldspar Porphyry, Moonta. Rutile Needles defining the edge of quartz grains within a phenocryst.(McBriar, 1962).*

Plagioclase has a slightly pink appearance due to the presence of submicroscopic particles of Fe-oxides; however under cross-polarised light they appear strongly twinned and are usually

relatively free from alteration products. However, when alteration products are observed, they usually consist of chlorite, sericite, hematite or quartz.

McBriar (1962) reported a small number of samples from the porphyry that also contained included phenocrysts of potassium feldspar. These are roughly the same size as the plagioclase phenocrysts but lack a clear crystal shape, are deeply corroded and contain abundant inclusions of plagioclase. Figure 4 in McBriar (1962) shows evidence of albitization of pre-existing K-feldspar, with albite occurring as a border to the K-feldspar.

Figure 4: Feldspar Porphyry- Normal Feldspar Porphyry, Moonta. Potash Feldspar phenocrysts that are highly albitised, corroded and deformed (McBriar, 1962, Kontonikas-Charos, 2013).

The porphyry groundmass in the majority of McBriar's samples constituted up to 80% of the sample by volume. The groundmass is made up of equal parts of microcrystalline aggregates of feldspar and quartz with a weak dissemination of chlorite fragments throughout. Grain size ranges from 0.02 to 0.05 mm and the grain boundaries are commonly laced with fine hematite (McBriar, 1962). The chlorite is relatively coarse and replaces primary biotite with small stringers of titanite

along cleavage planes. The chlorite is green, pleochroic, contains many pleochroic haloes around mineral inclusions and displays anomalous purple, green and grey interference colours. Euhedral granules of martite are often present in the groundmass.

However the porphyry does show a darker matrix in some areas, the colour is mainly dependent on the amount of chlorite and/or biotite in the groundmass. The colour varies from a dark purple to a dark black, and in which a well-defined cleavage or schistosity exists (McBriar, 1962).

Thin sections of this 'schistose porphyry' show great variation in the textures, aligned chlorite grains in a granoblastic matrix with grain size being roughly 0.025 mm. (Figure 5). It is within this Moonta Porphyry that the ore bearing lodes occur. The Moonta ore occurs in parallel series of lodes with a general NE-trending strike with a steep dip of around 40°-65° to NW. This country rock persists down to the deepest mine levels of 774 metres, and extends over an area of 44 km^2. The porphyry is, however, never exposed at surface (Jack, 1917).

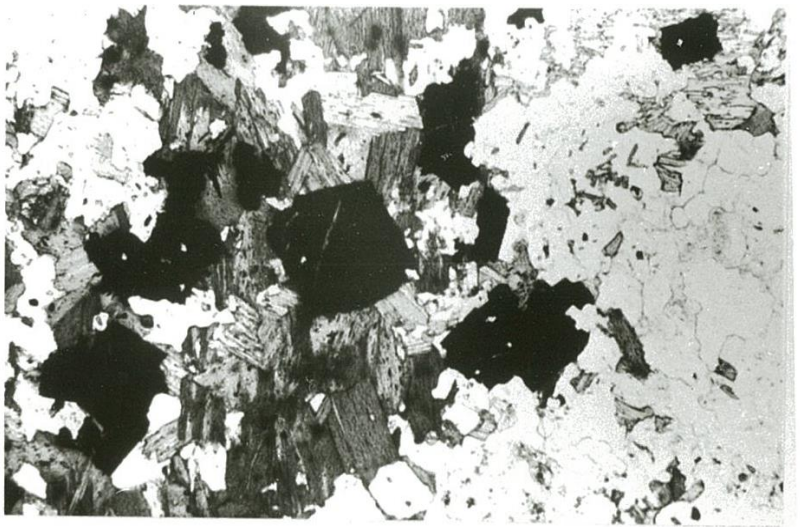

Figure 5: Quartz, biotite and martite (pseudomorphism of magnetite by hematite) crystals within the schistose porphyry in the Moonta region (McBriar, 1962).

Felsites

Jack (1917) referred to the term 'felsite' in his studies to describe this fine-grained crystalline rock, which is essentially non-porphyritic and generally similar in appearance to the groundmass of the feldspar porphyry. McBriar (1962) considered the felsite as a variant of the porphyry, and differentiated between the two.

The felsite is bright pink in colour with greenish-black mottling caused by chlorite content. The rock is quite brittle and fractures along the chlorite bands, the rock also contains scarce amounts of phenocrysts that occur as pink plagioclase or trace sulphides. The groundmass is composed of mostly quartz (35%), potassium feldspar and albite (65%) and ranges up to 1 mm in grain size. The groundmass has inclusions of rare perthite, which contains inclined albite (Figure 6). Like the porphyry, the felsite has small bands of chlorite and contains abundant disseminated titanite. Anhedral apatite is a common accessory mineral (Jack, 1917).

The felsite can further be altered into another lithological unit, *the schistose felsite*. Jack (1917) also described the unit as an interbedded/alternating layers of pale pink felsite and thin layers of green-black chlorite. Other minerals that also occur in this unit include; albite, potassium feldspar with accessory apatite. Porphyoblastic pink feldspars and trace sulphides are scarcely distributed throughout the unit.

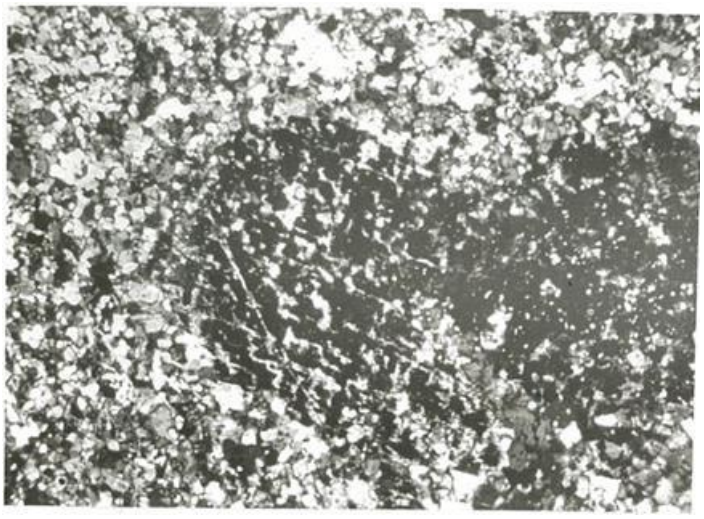

Figure 6: Potassium feldspar phenocrysts with regularly disposed albite inclusions within the 'Normal Felsite', Moonta (McBriar, 1962).

Metasediments.

The metasediments are a group of sedimentary-derived schists in the local area. Most samples in the area showed weak banding and foliation. The schist is composed of an assemblage of albite and biotite with alternating felsic and mafic layers with a scaly lepidoblastic texture. The light layers of the schist are mostly composed of quartz with albite-feldspar and biotite making the rest of the layer. The biotite shows slight replacement by chlorite, lending the rock a slight greenish colour. The dark layer is generally richer in biotite and generally lacks albite. Flaky red oxidized hematite can persist along the boundaries of the layers. The average grain size is roughly 0.05 mm (McBriar, 1962).

APPROACH AND METHODOLOGY

Twenty hand specimens from McBriar (1962) were selected to be remounted as one-inch polished blocks (Table 1). The majority of these comprise massive sulphides (<80% sulphide material), and are considered to be representative of copper ore mined in the Moonta area. Most came from the Moonta mine, with a minority of samples from the Wallaroo Mine for comparison.

Scanning Electron Microscopy

An FEI Quanta 450 scanning electron microscope (SEM) with energy dispersive X-ray spectrometry and back-scatter electron (BSE) imaging capabilities (Adelaide Microscopy, University of Adelaide; AM-UoA) was used. BSE imaging (accelerating voltage, 20 kV, and beam current of 10 nA) allowed for characterization of each sample in terms of significant textures and mineralogical relationships.

Reflected Light Microscopy

An Nikon Eclipse LV100 POL Petrographic Microscope was used to capture high resolution images under advanced polarized light at both diascopic and episcopic illumination capabilities (Adelaide Microscopy, University of Adelaide; AM-UoA).

RESULTS

Petrography

The investigated samples (Table 1) belong to the system Cu-Fe-S. The main sulphides are bornite, chalcopyrite and pyrite; minor amounts of covellite and chalcocite were also present. These assemblages are the products of hypogene IOCG mineralization, although some samples display evidence of secondary oxidization and alteration. Traces of hematite and albite are present and belong to the hypogene mineral assemblage.

Sample ID	Main mineral	Sulphides Present			Other Minerals	Accessory Minerals				Location/Area
		Cpy	Bn	Py		Ti	Hm	Mt	Ru	
5045	Pyrrhotite	X		X	Po, Qtz,Bt,Hb,Ap					Wallaroo Mines
162/8	Chalcopyrite/Bornite	X	X		Ksp, Qtz,		X			Moonta Mines
162/9	Chalcopyrite/Bornite	X	X		Qtz					Unknown
162/10	Chalcopyrite/Bornite	XX	X		Qtz					Moonta Mines
162/11	Bell Metal Chalcopyrite	XX		X	Ap, Qtz, Ma					Moonta Mines
162/12	Chalcopyrite	X								Wallaroo Mines
162/14	Chalcopyrite	X								Wallaroo Mines
162/49	Cobaltite	X		X	Cb, Ca, Bi, Cal					Wallaroo Mines (Hall's Shaft)
162/53	Sphalerite	X		X	Sph, Cal					Wallaroo Mines
162/56	Bornite	XX	X			X	X	X		Moonta Mines
162/57	Bornite	XX	X							Moonta Mines
162/58	Bornite	XX	X					X		Moonta Mines
162/59	Bornite	XX	X		Ur		X	X		Moonta Mines
162/60	Bornite	X	X		qtz					Moonta Mines
162/65	Covellite		X	X	Cv, Qtz				X	Moonta Mines
162/66	Covellite		X	X	Cv, Orth	X			X	Moonta Mines
162/104	Pyrrhotite	X		X	Pyrr,Qtz, Bt,Hb					Wallaroo Mines
162/106	Hematite	X		X	Qtz		X			Moonta Mines (Yelta)
162/109	Hematite	X		X	Qtz		X			Moonta Mines
162/110	Ferberite				Fer					Wallaroo Mines

Abbreviations: Ab – albite, Act – actinolite, Ap – apatite, Bast – bastnasite, Bi – Bismuth, Bn – Bornite, Bt – biotite, Cal – calcite, Cb – Cobaltite, Cpy – chalcopyrite, Chl – chlorite, Cv -Covellite, Fer – Fererite, Hm – Hematite, Il – ilmenite, Ksp – K-feldspar, Ma – Malayaite, Mon – monazite, Mt – magnetite, Mu – muscovite, Orth – Orthoclase, Plag – plagioclase, Py – Pyrite, Po – Pyrrhotite, Ru – rutile, Ser – sericite, Sph - Sphalerite, Ti – titanite, Ur – Uranium, Xen – xenotime, Zrc – zircon,

Table 1: The list of samples analyzed with the SEM scanner at Adelaide Microscopy

Bornite

The bornite in the Moonta ores is typically massive. The bornite-dominant samples are heavily fractured in some areas (Figures 7a, 8a and 9b, c). In others, however, fractures are absent, suggesting that part of the bornite mass may have recrystallized after deformation.

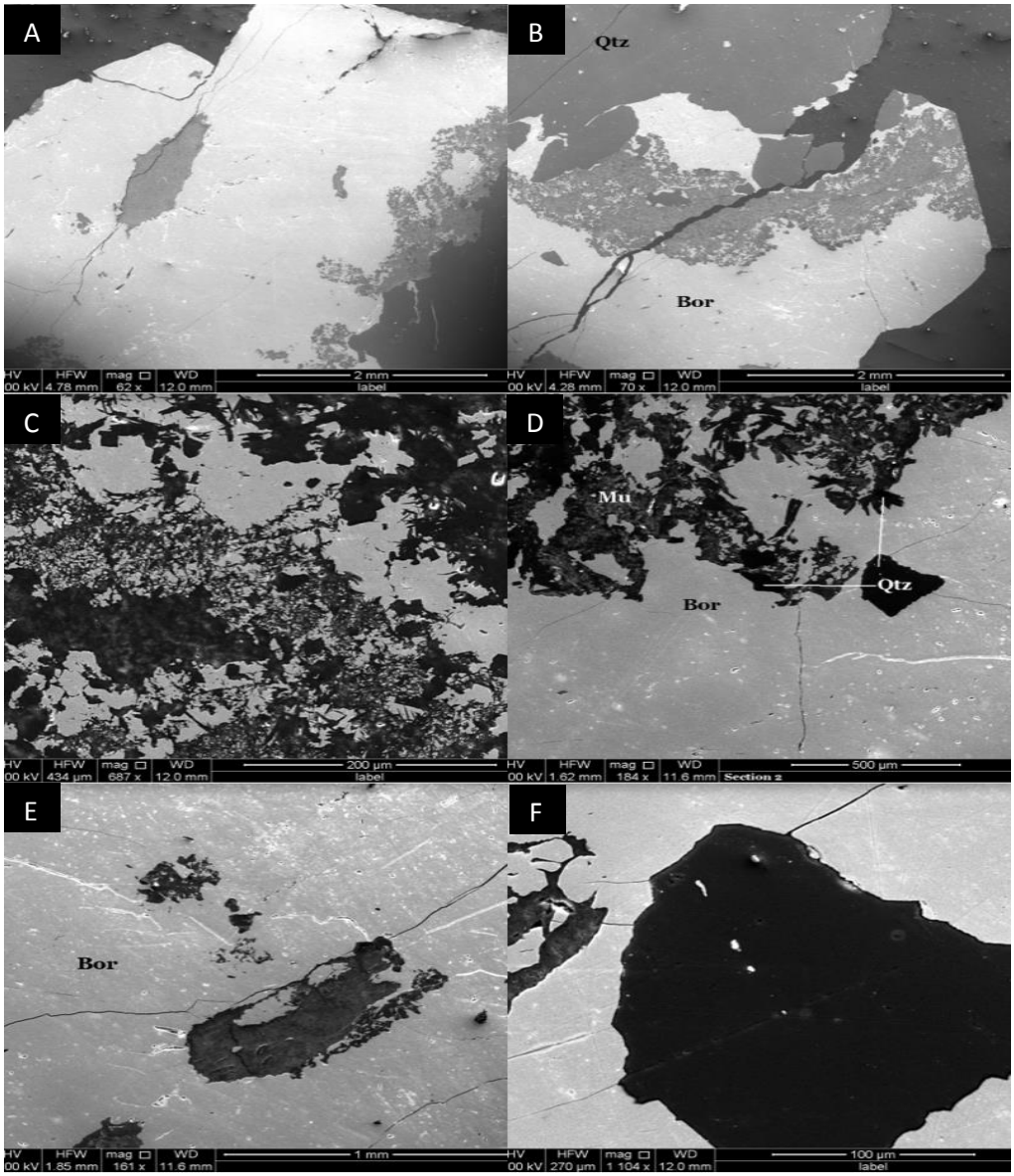

Figure 7: *Sample 162/60 – Bornite Sulfide: (a) Overall Relationship of Quartz and Bornite, (b) Hematite growth in the Bornite does not enter into the quartz dominated areas, (c) Aluminosilicates, quartz almost attack the bornite sulfide, (d) Quartz grains impure the bornite dominated mineralization, (e) Tarnish within the bornite, (f) Quartz phenocryst within the bornite.*

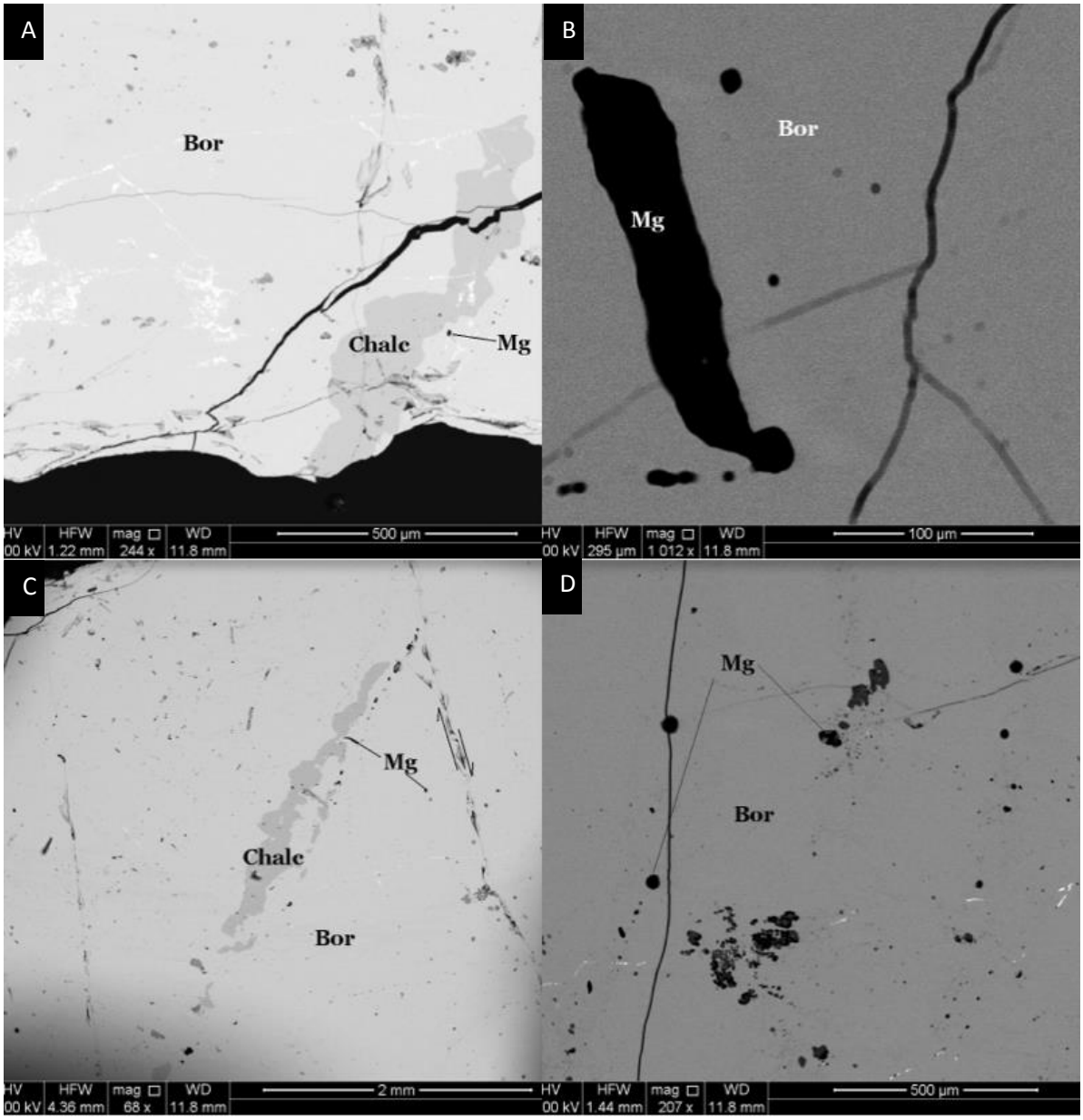

Figure 8: *Sample 162/58 – Bornite Sulfide: (a) Large groundmass of bornite shows pseudo growth of chalcopyrite before a stress event causing large fracture plains, (b) Magnetite grains as large as 200µm in length are abundantly common throughout the Bornite-rich matrix, (c) Chalcopyrite sulfide growth tends to be in elongate linear trends, commonly along fractures (ie. Arrows demonstrate), (d) Magnetite grains tend to grow in clusters and are commonly located close together in distinct areas*

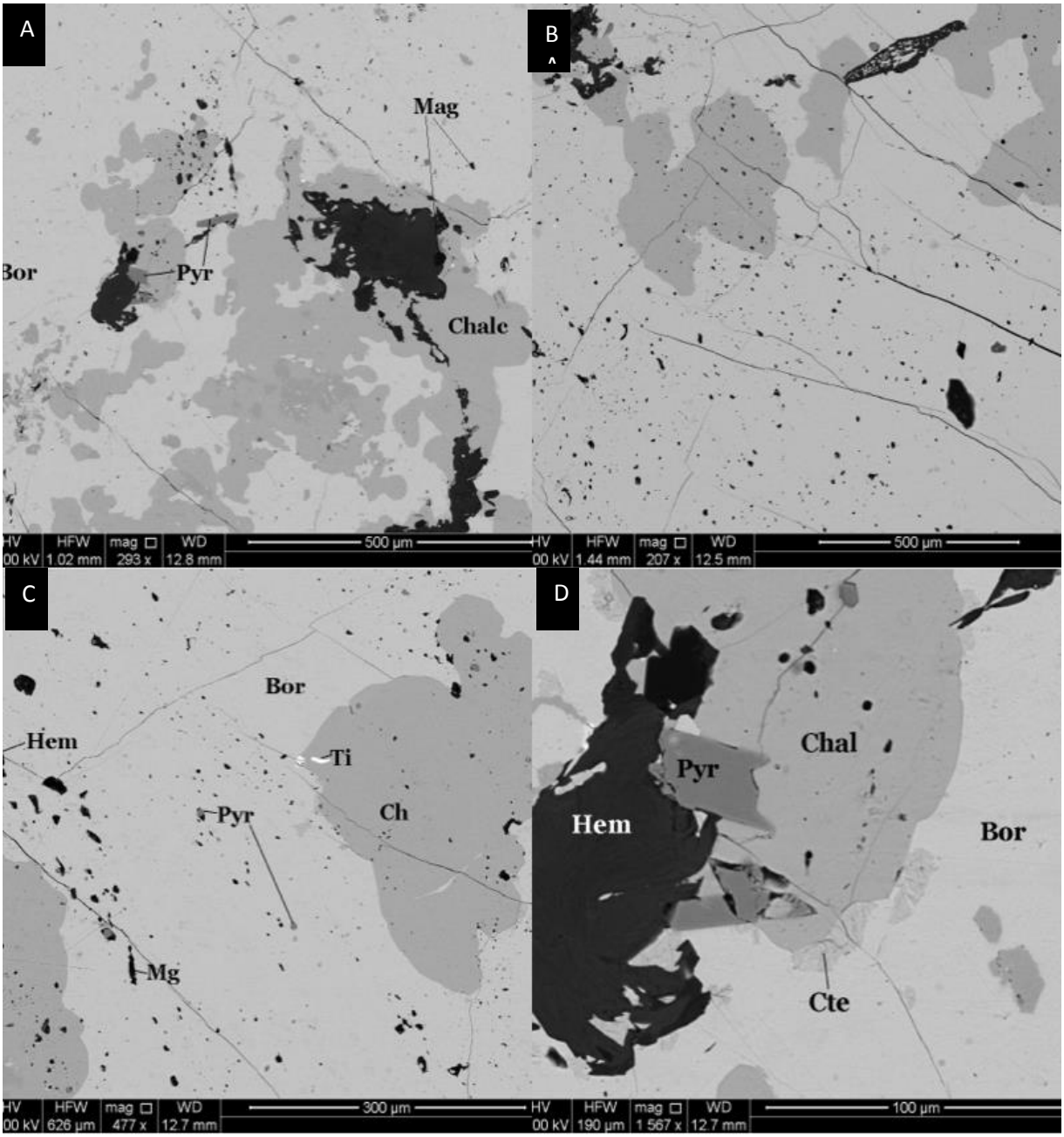

Figure 9: *Sample 162/56 – Bornite Sulfide: (a) Groups of mineralization occur within the Bornite matrix, typically abundant chalcopyrite and magnetite grains occur, aluminosilicate gangue minerals are commonly surrounded by the chalcopyrite growth, (b) Heavily fractured areas are common throughout the Bornite sample, (c) Rare inclusions of Titanite (sphene) and Hematite occur, titanite commonly associated with the chalcopyrite, (d) Pyrite grains are common throughout the groupings of vast mineralization (zoning areas), Small grains of Chalcocite are common in Iron depleted sections.*

Bornite makes up as much as 80% of the bornite-dominant samples. Lesser amounts of accessory chalcopyrite are present. Smaller amounts of quartz and magnetite are abundant throughout the bornite. Some samples are characterized by abundant hematite. This hematite is closely intergrown with the bornite, and appears to be paragenetically later, such as the sample 162/59 (Figure 10c).

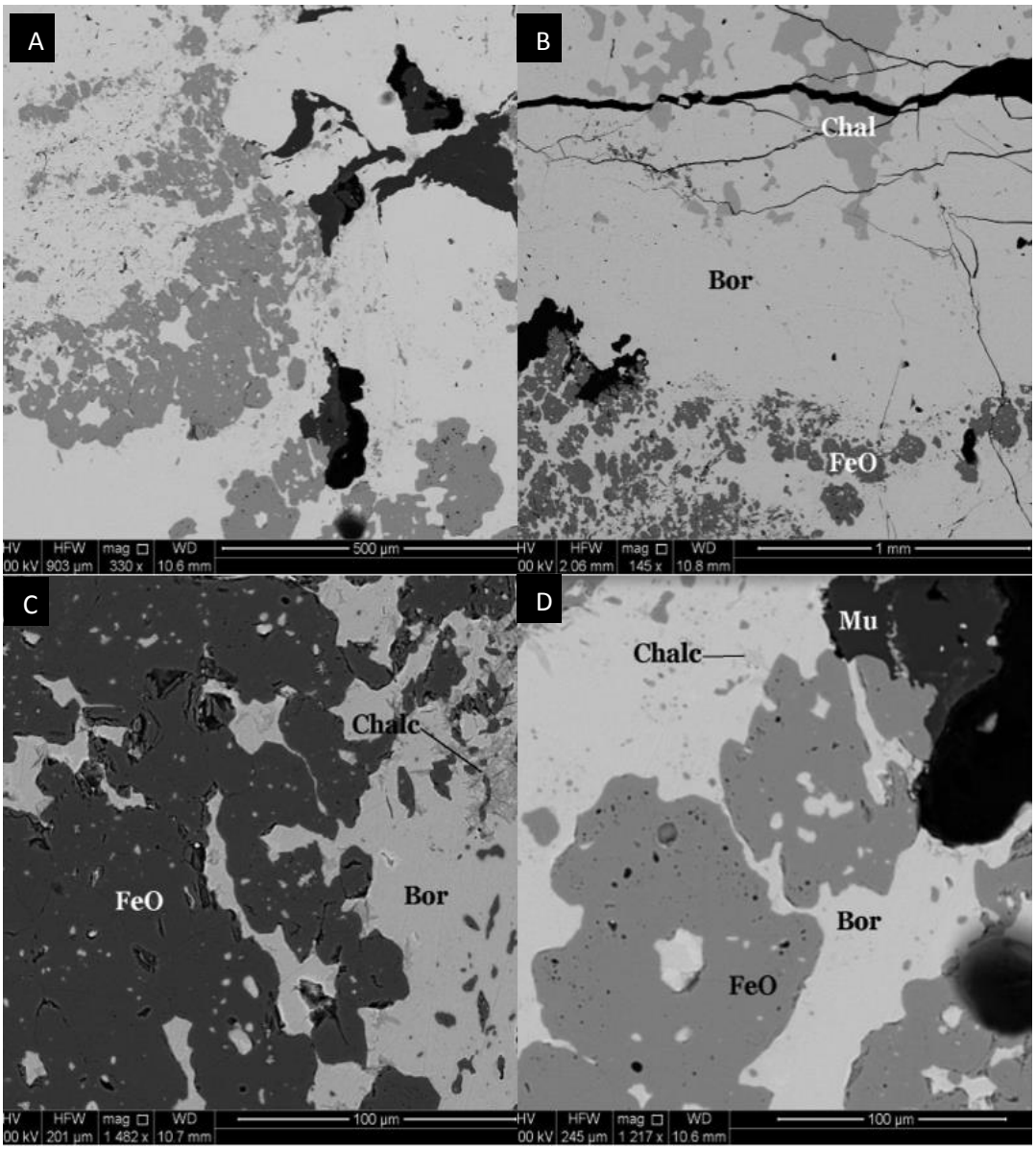

Figure 10: *Sample 162/59 – Bornite Sulfide: (a) Sample is dominated by a bornite background with mineral growth of Hematite, Muscovite and Quartz, (b) Bornite groundmass interacts with hematite and chalcopyrite mineralization, (c) Hematite mineralization includes macroscopic*

inclusions of bornite, (d) Hematite mineralization includes macroscopic inclusions of bornite

Magnetite is observed to be scattered through sample 162/58, Grain size does not exceed 200 µm in diameter and the grains are typically clustered (Figure 8d). There is a strong relationship between magnetite and hematite in that they are commonly found together as seen in sample 162/56, (Figures 9a, d). There is, however, no clear indication of whether one Fe-oxide has replaced the other. In hand specimen, bornite is commonly a blue-purple 'peacock' colour that can be altered by weathering into covellite, which can also be seen at the microscopic scale.

As well as occurring in massive form, bornite also occurs within veinlets, aggregates in large chalcopyrite-dominated samples, and replacing other sulphides. Jack (1917) considered that although the bornite is a primary sulphide, bornite, it might nevertheless have been involved in processes of secondary sulphide enrichment. Jack described the bornite as 'enwrapping', thus being a later mineralization event than the chalcopyrite. This observation can be regarded as truly visionary as it predated modern concepts of re-equilibration, remobilization and recrystallization of sulphides by at least seven decades! In the present sample suite, there is abundant petrographic evidence for later re-equilibration, and for multiple 'generations' of bornite. There is, however, also contradictory evidence. Sample 162/08 (Figure 11a) shows evidence that the bornite was the primary sulphide and is replaced by chalcopyrite, in other cases, chalcopyrite appears paragenetically earlier, especially within the 'Bell-Type' Chalcopyrite (*explained below*). The common contradictions in mineral relationships are a feature shared by other South Australian IOCG ores and are highly suggestive of

repeated cycles of sulphide crystallization and recrystallization over a prolonged period. Hand specimens examined also show evidence of replacement of chalcopyrite by bornite.

The bornite specimens examined tend to display conchoidal fracture and tarnish a purple-blue colour. Thy can also be somewhat brittle; this is partially due to weathering from oxidization. Rarely a certain degree of crystallinity is revealed by the very weak anisotropy, and occasionally there is secondary alteration to covellite or, less frequently, to chalcopyrite. McBriar (1962) explains that, in one instance, alteration to a bright blue mineral believed to be digenite was observed (McBriar, 1962). This would be consistent with the same reaction in other IOCG ores such as Olympic Dam and Prominent Hill. In sample 162/56, bornite-dominant massive sulphide shows iron-depleted areas in which small chalcocite grains occur (Figure9d).

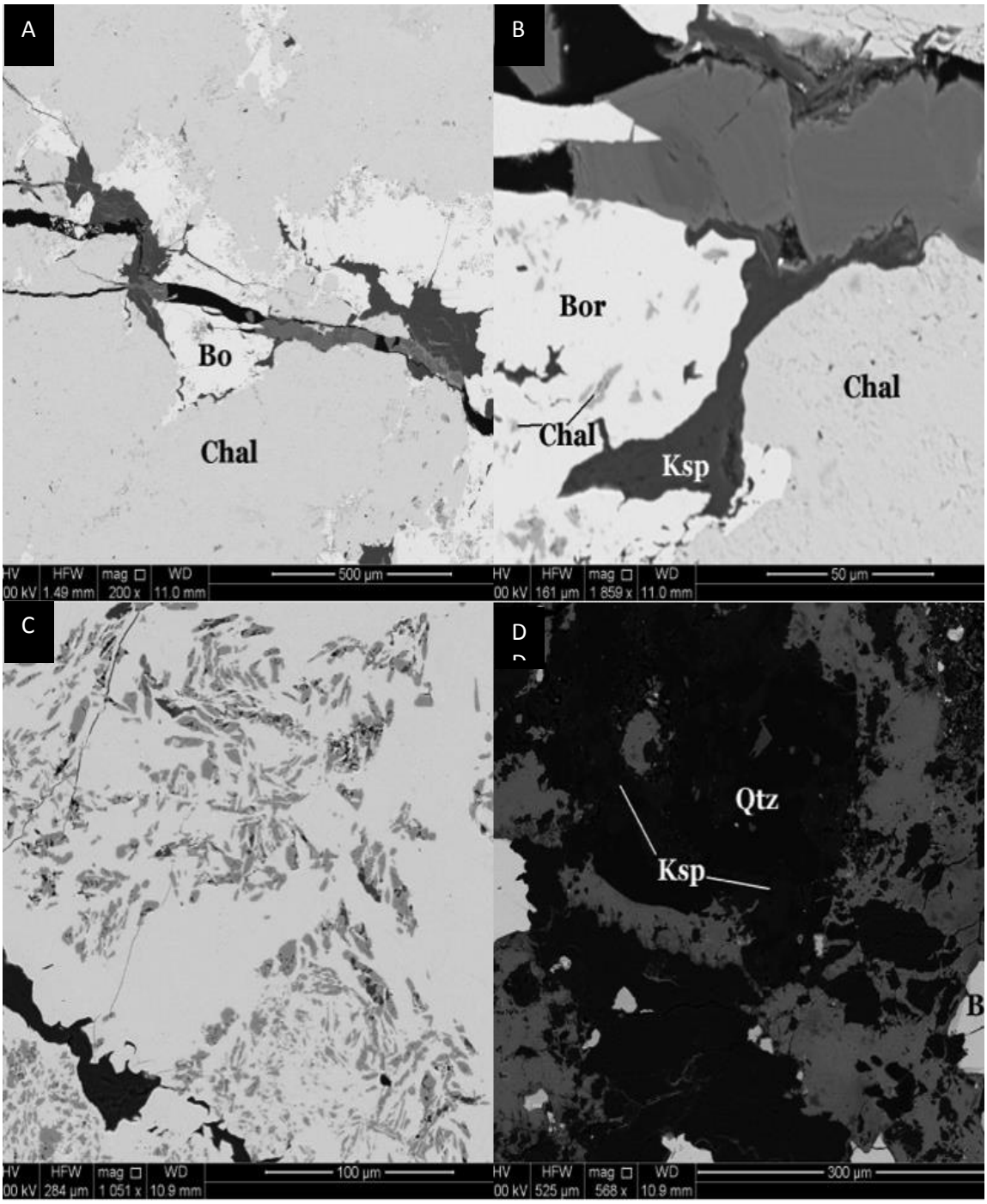

Figure 11: *Sample 162/08 – chalcopyrite/bornite: (a) Fractures within the sulfides are infiltrated by potassium feldspar and hematite, (b) A close up of the fracture shows the mineralization that as grown within the empty void, (c) Bornite is inhabited by small granules of hematite, (d) The gangue in this sample is made up predominantly of k-feldspar and quartz that are making up the darker area of the gangue, whilst the hematite makes up the grey area, constituting around 40% of the total gangue.*

Chalcopyrite

Chalcopyrite examined in reflected light and by SEM showed a wide variety of grain sizes shapes and also colours. McBriar (1962) split chalcopyrite into three distinct groups; (1) Euhedral – "Pure"; (2) Massive – fine-grained or "bell metal" type; and, (3) Massive – coarser-grained or "bright" type. Chalcopyrite is the most abundant copper sulphide in the Moonta-Wallaroo Region and is usually associated with most other sulphides.

Chalcopyrite samples analysed by SEM were largely pure, impurity-free 100% chalcopyrite grains. For this reason, this type of chalcopyrite will be referred to here as 'pure'. Chalcopyrite in these samples is euhedral and typically massive (grains can exceed over 2 mm in size). The euhedral crystals have a perfect tetragonal wedge-shape in cross-section (Figure 12a). Chalcopyrite-dominant samples are, however, somewhat fractured without evidence for inclusions of any mineral inclusions.

These findings are consistent with those of McBriar (1962) who sent a chalcopyrite sample (162/18) for analysis which returned no trace of impurities apart from 2-5 mm-sized grains of pyrite surrounded by marcasite. Samples taken from the Moonta mines generally have few associated minerals, thus contrasting with samples from the Wallaroo mines, which are associated with chlorite. Indeed, chalcopyrite samples from Wallaroo tend to display a 'rough euhedral' morphology and may attain up to 2.5 cm in size. They are also slightly tarnished, deeply striated, and may occur within nests of slim quartz crystals sometimes covered with fine shavings of specular hematite.

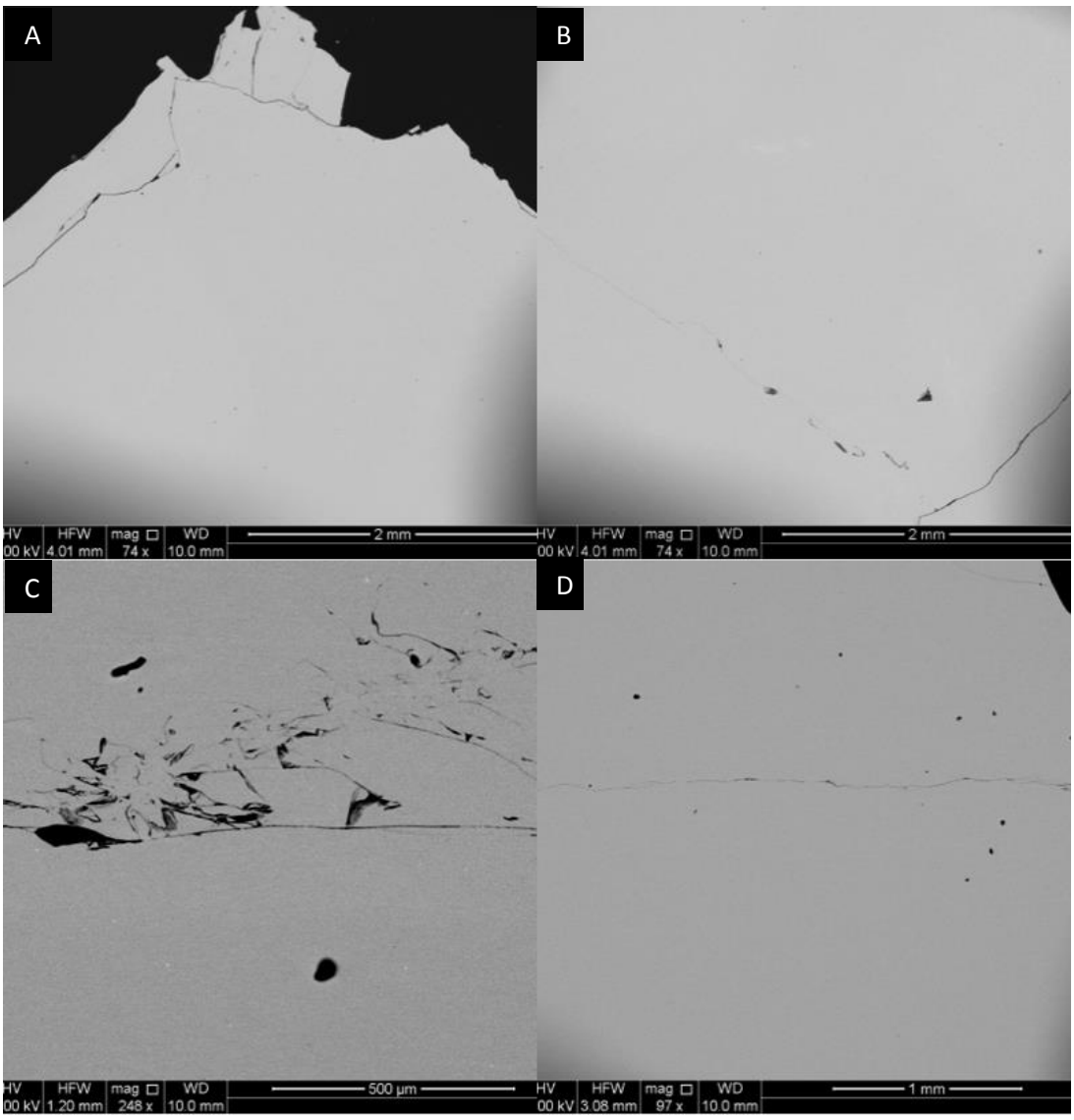

Figure 12: *Sample 162/12 and 162/14 – Chalcopyrite: (a) 'Pure type' Chalcopyrite, 100% complete chalcopyrite, (b) Another view of the 100% chalcopyrite, (c) deformation structures within the 'pure-type' chalcopyrite, (d) fracture lines within the chalcopyrite.*

The second variety of chalcopyrite (massive fine-grained, or "Bell-Type" chalcopyrite) is more abundant in samples from the Moonta mines area. This sub-type differs from that of the 'pure-type' by rapid tarnish to a dark yellow/brown colour, The bell-type chalcopyrite also tends to fracture erratically, i.e., fractures does not take place along common planes and tends, instead, to display a conchoidal fracture network. It is,

however, similar to the 'pure-type' chalcopyrite in that it commonly occurs alone without any inclusions. It also occurs as aggregates of irregular size and shape within a matrix of coarse crystalline chalcopyrite or in a bornite-chalcopyrite groundmass (Figure 8c). Bell-type chalcopyrite can contain microscopic inclusions of bornite, magnetite, pyrite, hematite and gangue minerals (mostly aluminosilicates) but these are rarely consistent across the sample suite, making it difficult to constrain mutual relationships (Figure 13c).

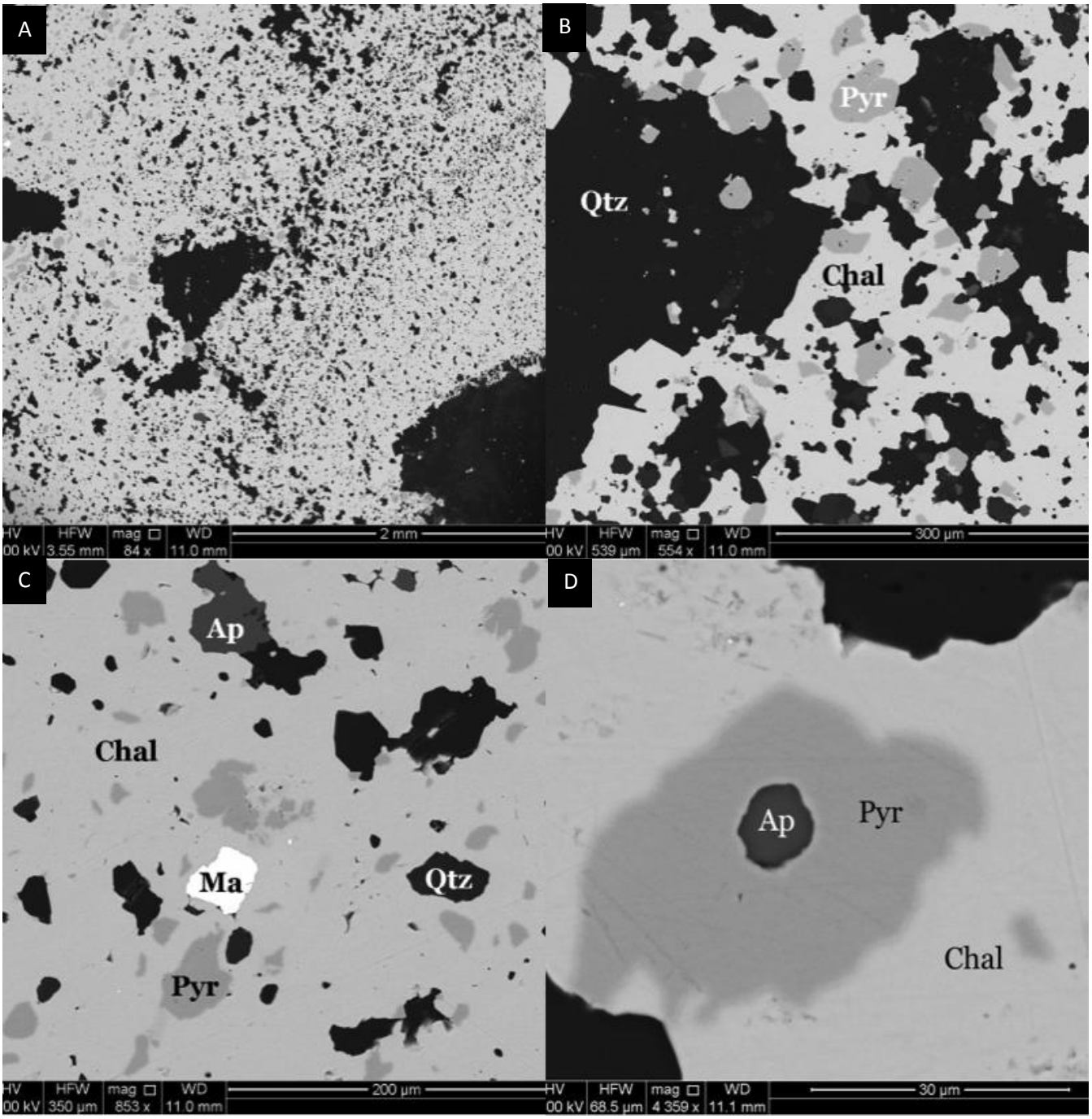

Figure 13: *Sample 162/11 – Chalcopyrite (Bell Metal): (a) Image shows the general distribution of the chalcopyrite with gangue grains and tiny pyrite inclusions, (b) Bell Metal chalcopyrite is effected by anhedral pyrite inhabitants, (c) Bell Metal chalcopyrite contains rare inclusions of apatite and what is interpreted as Malayaite (An Sn bearing Hydrothermal alteration of cassiterite-quartz assemblage and Sn-bearing skarns. Structurally related to titanite.), (d) Tiny rare inclusion of apatite within a 30um pyrite grain within the bell-metal chalcopyrite*

McBriar (1962) showed one aspect of 'Bell-Metal' chalcopyrite via an acid dissolution experiment. The residue consisted of two types of quartz and a dark mineral. The dark mineral was described as a decomposed chlorite, while the two types of quartz were considered as a pink-coloured vein type, full of microscopic "dusty" inclusions of iron oxide, whereas the second was very clear, comparable to that in the Moonta porphyry (McBriar, 1962).

The third and final type of chalcopyrite observed in the Moonta-Wallaroo sample suite was the massive, coarse-grained 'bright-type'. It is the most common type of chalcopyrite observed in samples from both the Moonta and Wallaroo region. At Moonta, 'bright' chalcopyrite is intimately associated with bornite, martite, pyrite and molybdenite, where in Wallaroo it is commonly associated with pyrrhotite, pyrite and sphalerite (Figure 14c). The 'bright-type' chalcopyrite tends to be containing an abundance of mineral inclusions, dominated by microscopic pyrite.

In some instances, chalcopyrite shows an exsolution of tiny bornite granules (Figure 15a-d). These granules are typically aligned in linear arrangement and tend to be restricted to certain areas of the host chalcopyrite grain.

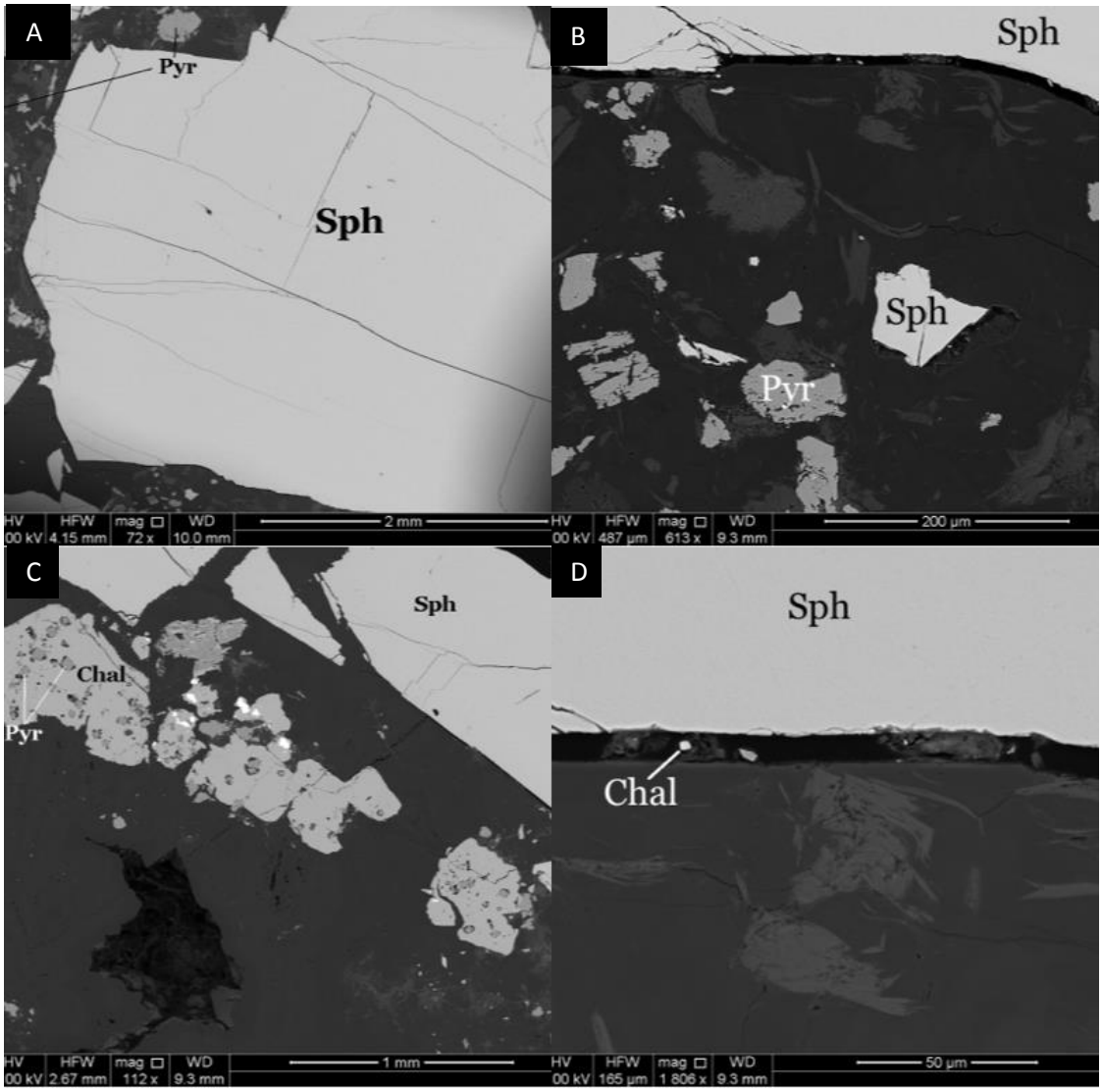

Figure 14: *Sample 162/53 – Sphalerite Sulfide: (a) Sphalerite grains are massive and euhedral, grains extend up to 3mm in size, (b) The matrix is made up of some sort of aluminosilicate, darker areas are presumed to be calcite as they are high in calcium, where they grey gangue mineral is calcium depleted. The matrix is host to small phenocrysts of pyrite and Sphalerite grains, (c) Chalcopyrite is common throughout the sample as anhedral grains that plays host to pyrite inclusions, (d) Where the Sphalerite grains meet the matrix there is a defined border of calcium enriched aluminosilicate that also hosts to small chalcopyrite and pyrite grains.*

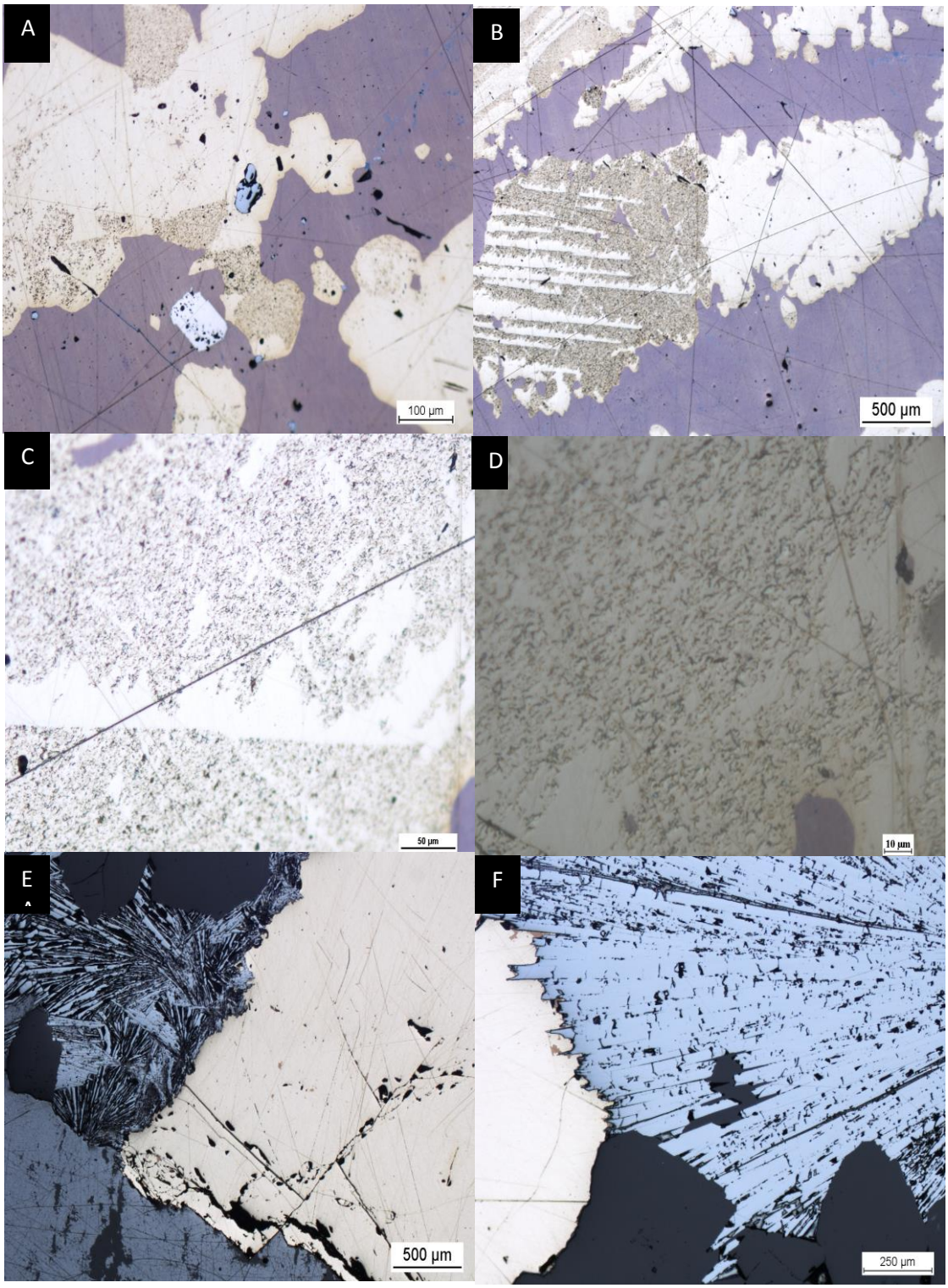

Figure 15: *Sample 162/10: (a-d) Reflected light photomicrographs showing exsolution of tiny bornite granules within chalcopyrite. The excreted bornite tends to have a linear distribution, following crystallographic planes in the host mineral. (e and f) Relationship between hematite and chalcopyrite suggestive of later overgrowth.*

Hematite

Hematite, the iron oxide is present in a lot of the ore-containing samples located from Wallaroo, more importantly for this study, it is even more so abundant in the Moonta located samples. The Hematite in the Moonta area is largely associated with the bornite-dominated sulphides as seen in SEM images from sample 162/59 (Figure 10a). Hematite occurs in a couple of varieties within the Moonta-Wallaroo sample suite, in Figure 11c, hematite occurs as oval shaped grains in the bornite dominated groundmass. Hematite, under reflected light shows very sharp needle-like grains that cut into the surrounding minerals. Figure 15e-f demonstrates the distribution of the needle-like grains. In the figure, hematite overgrows the aluminosilicate gangue mineral and further grows into the fractured area.

Pyrite

The Moonta-Wallaroo region consists of many accessory minerals, in terms of pyrite, it is customarily common to have relations with chalcopyrite, however also exhibits strong relationships with bornite, pyrrhotite, sphalerite, galena and cobaltite. In most of the chalcopyrite samples, pyrite occurs as inclusions or as euhedral grains in the sample. The only exception is within the 'pure-type' chalcopyrite where the sample is impurity free, Pyrite occurs in both the 'bell metal' and 'bright' type chalcopyrite. Pyrite was witnessed to have two different grain shapes, one, a distinct sharp-edged euhedral grain, the other a rough, soft-edged anhedral grain, amazing both witnessed in the one sample close together in Figure 16. In this occasion the euhedral pyrite is an inclusion

mineral within a grain of chalcopyrite in a sphalerite-dominated ore, whereas the anhedral pyrite mineral is a free grain within the gangue matrix. The euhedral-grained pyrite frequently exhibits a cubic form with perfectly polished faces.

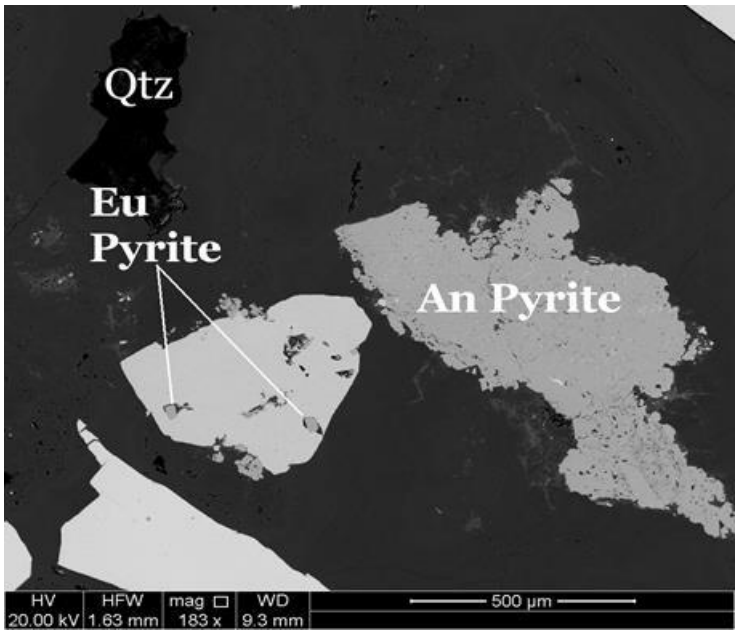

Figure 16: Sample 162/53 (sphalerite): Two distinct pyrite morphologies co-exist. There are smaller Euhedral grains (Eu) that often occur as inclusions within chalcopyrite, and anhedral grains (An) that are observed outside of the chalcopyrite within gangue quartz.

Pyrrhotite

Pyrrhotite is a major sulphide in the Wallaroo ores; it is much less common in the Moonta subdomain. The pyrrhotite-dominant sample examined here displayed great variety in grain size. Coarse pyrrhotite is crosscut by fractures, which contain hornblende and smaller grains of apatite granules (Figure 17 a). Overall, this sample is quite deformed showing stress evidence in fractures. Pyrrhotite is hosted within the same aluminosilicate gangue groundmass as the other sulphide samples. Small grains of chalcopyrite and quartz also occur within gangue, the aluminosilicate also hosts anhedral, porous hematite with a 'swiss cheese'-like appearance. Hornblende within

pyrrhotite also contains inclusions of a second Fe-Si-O-Al-Mg-Ca-bearing mineral as elongate stringer veins (Figure 17 b).

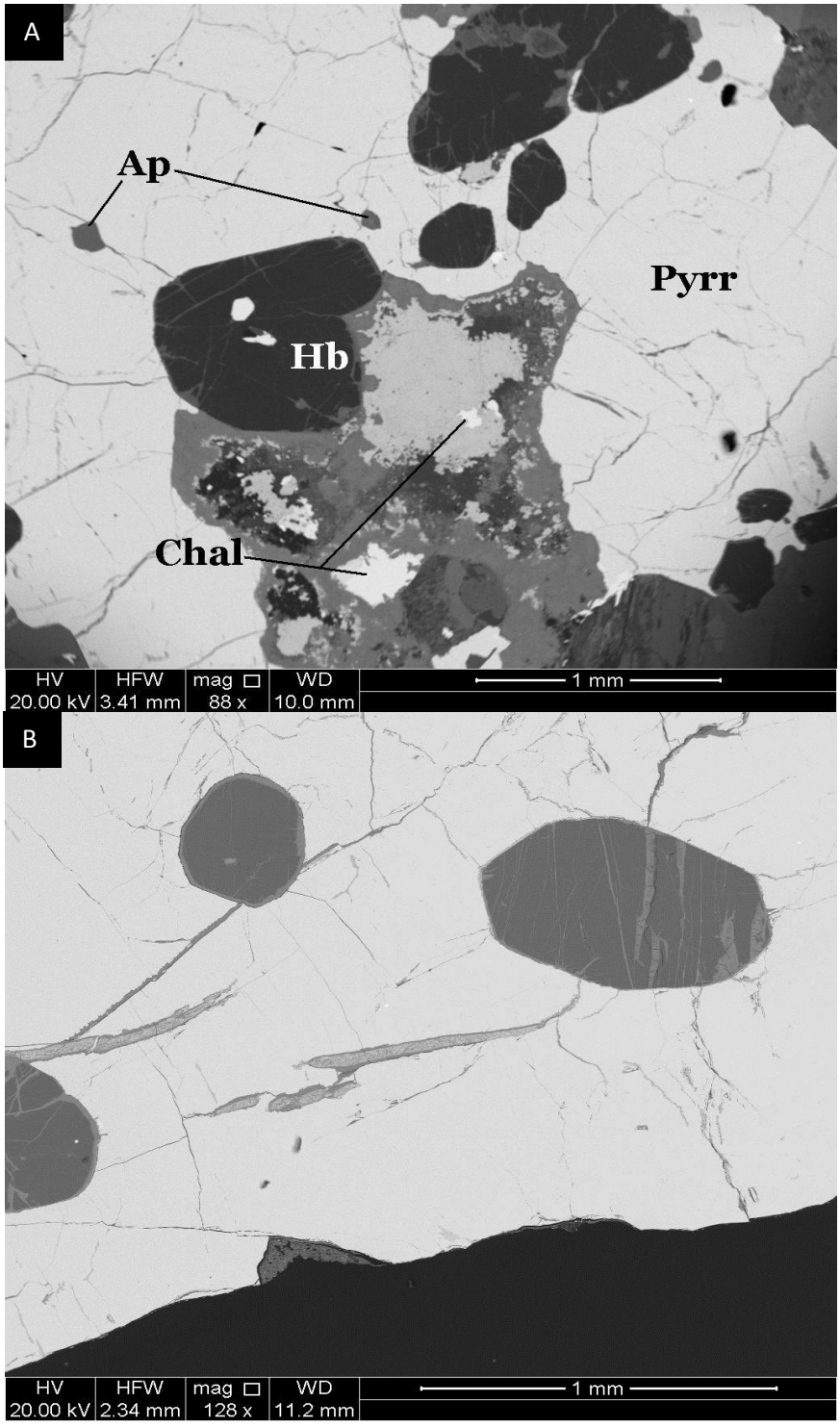

Figure 17: (a) *Sample 162/104 – Pyrrhotite: Fractured Pyrrhotite hosts many inclusions, majorly being hornblende and apatite, (b) Sample 162/104 – Pyrrhotite: Elongate stringer grains within the Pyrrhotite are rich in Malaynite*

Other Minerals

Magnetite, when in occurrence is observed in relict material enclosed within the hematite of martite crystals and is very isolated from the sulphide minerals. The samples showed evidence that wherever an iron oxide is in contact with the neighbouring sulphide, the oxide mineral was always hematite. According to McBriar (1962) phase equilibrium studies, wherever bornite is absent, both hematite and magnetite can coexist with chalcopyrite and pyrite, and magnetite is stable with chalcopyrite, pyrite and *p*yrrhotite.

Only one sample of cobaltite was analysed in the sample suite, the sample was located from Hall's Shaft in the Wallaroo Mines. The sample distinguished a poikilitic texture of cobaltite, a pink-silver colour in hand specimen within a quartz-feldspar dominated rock. The SEM produces some interested mineral textures with the cobaltite grains being heavily deformed and fractured. Within these fractures, mineral growths of chalcopyrite and quartz grains are witnessed along with significant gangue aluminosillicate infill (Figure 18c). The aluminosillicate gangue has a calcium rich/calcium poor mix, the lighter grey areas of the gangue matrix (Figure 18c) contain the higher content of calcium, whereas the lighter areas contain almost no calcium. The cobaltite grains within the rock are actually quite rare but are large in size when found, the grains are well formed, euhedral in shape and commonly associated with large euhedral pyrite grains. Native bismuth is scarce, but occurs commonly along the boundaries of pyrite grains (Figure 18a).

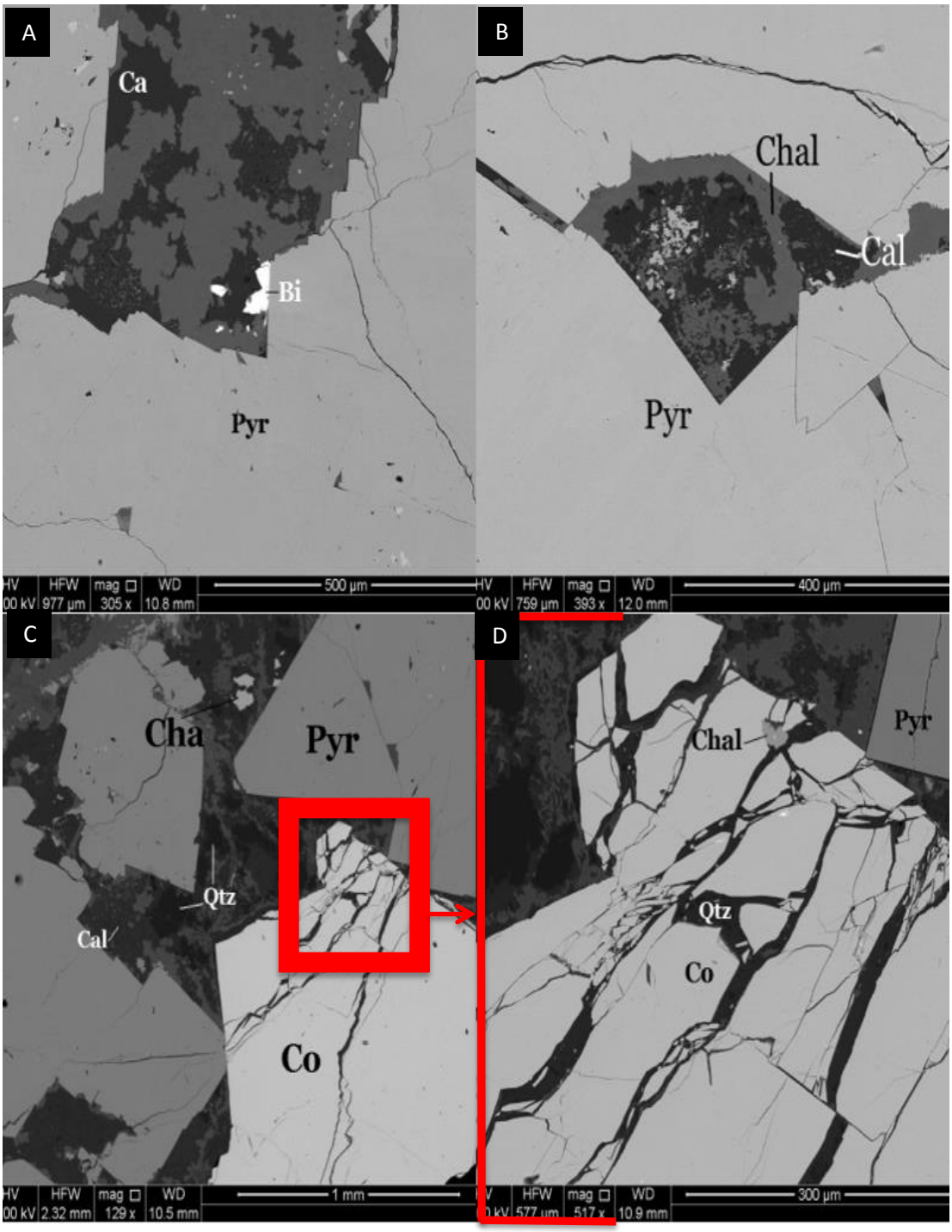

Figure 18: *Sample 162/49 – Cobaltite Sulfide: (a) Sample is dominated by abundant Pyrite with a rare native Bismuth granule no bigger than 50µm, gangue matrix is composed of Calcite and other aluminosilicates (b) Fractured areas within the Pyrite can sometimes contain chalcopyrite mineralization along with the Calcite gangue, (c) Cobaltite grains are scarce but large in size (1-2mm), the grains are euhedral and heavily fractured. Pyrite grains are also euhedral and similar in size, however can range from 20µm-1.5mm, (d) Within the fractures of the Cobaltite, quartz mineral growth has occurred along with the odd chalcopyrite granule.*

In the Moonta region, bornite has been altered into a deep purple covellite. SEM imaging explains a sharp needle texture from the covellite that tends to grow around large gangue minerals. A good example is shown as Figure 19e (sample 162/66) in which a large grain of orthoclase that has been surrounded by covellite needle mineral growth. REE are found within this altered sulphide, titanite, or yet sphene, a calcium titanium nesosilicate can be found in the mix of deformed quartz groundmass (Figure 19f). Tiny rutile grains are also found in a less deformed quartz groundmass, no real relationship is defined with the rutile, it just grows scarcely erratically within the quartz (Figure 19c). Macroscopic euhedral grains of pyrite are located in covellite-dominated areas of sample 162/66 and 162/65 (Figure 19d).

Sphalerite was located only in the Wallaroo region and was commonly associated with smaller grained galena. Sphalerite grains are large, frequently over 2 mm in size and displays fractures in two orientations. Fractures are perpendicular to one another and extend through most of the mineral (Figure 15a).

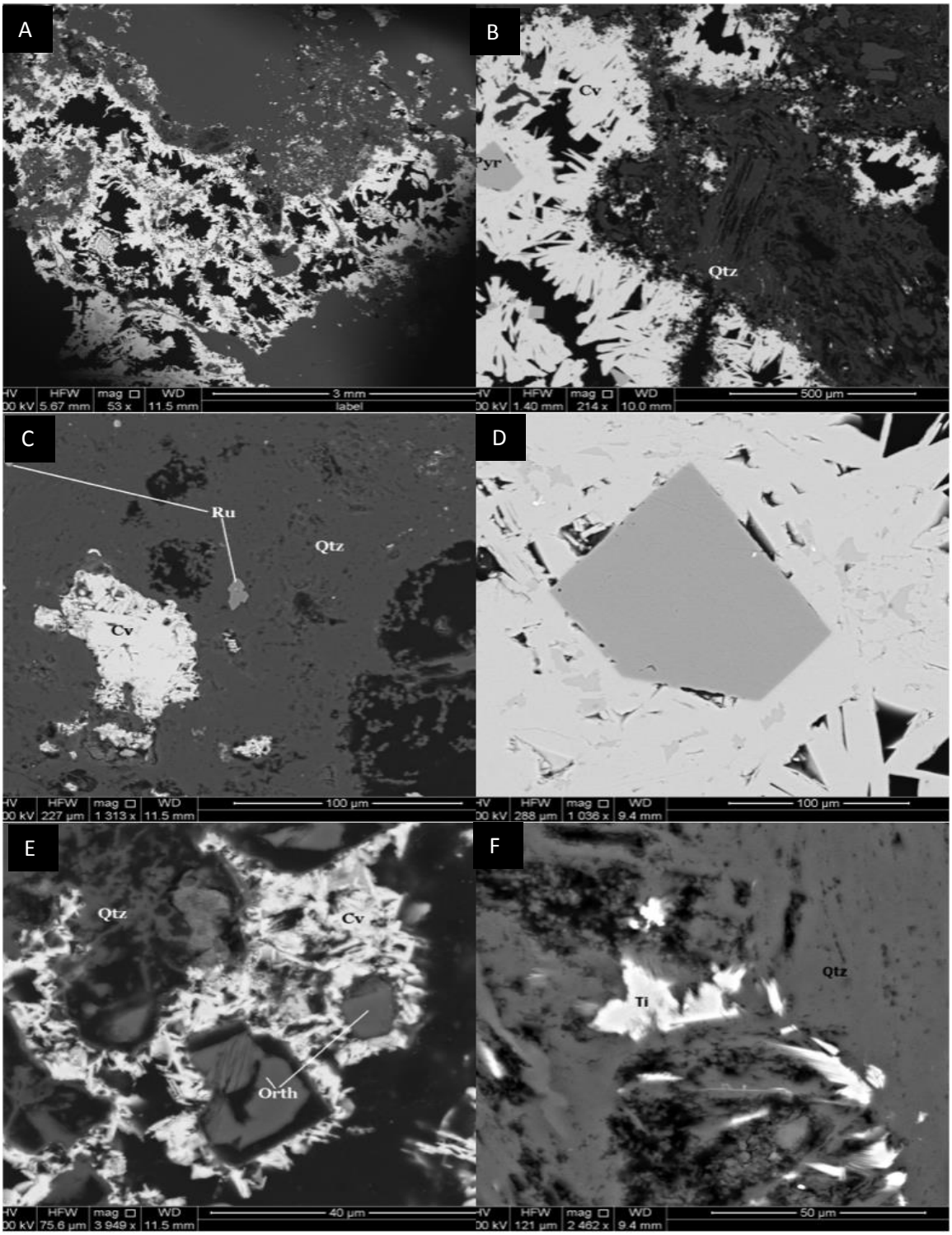

Figure 19: *Sample 162/66 (Covellite): (a) The overall texture of the sample in which covellite needles growing within quartz gangue, (b) Deformed quartz is surrounded by covellite needle boundary with inclusions of pyrite, (c) scarce amounts of microscopic rutile within quartz, (d) Pyrite grains range up to 150 µm in diameter within covellite, (e) Rare grains of orthoclase enclosed by covellite, (f) Inclusions of titanite within the deformed quartz groundmass.*

DISCUSSION

Conditions of ore formation

Prior to this study, no contemporary ore mineralogical study existed of the massive copper ores in the Moonta and Wallaroo Mines. Accordingly, there are few available constraints on the temperature of formation, the composition of ore-forming fluids, or other parameters that could help develop a genetic model for the deposits.

The single published study of relevance is that of Morales-Ruano et al. (2002). These authors were able to recognize four hydrothermal stages separated by episodes of fracturing. The first two stages were dominated by Fe-oxides (dominantly magnetite), the third by Fe-sulphides (pyrite and pyrrhotite) and the final stage by an assemblage comprising Cu-(Fe)-sulphides (+cobaltite, sphalerite and galena). Morales-Ruano et al. (2002) examined fluid inclusions in quartz associated with oxide and sulphide minerals, and established three distinct types. The first is a two-phase, vapour-rich type, with homogenization temperatures up to 473 °C and salinity of 2-22 wt.% NaCl equivalent. Type-2 inclusions are two-phase liquid-rich with lower homogenization temperatures (up to 269 °C) and lower salinities (0.7 to 22 wt.% NaCl equivalent). Type 3 are liquid-rich inclusions with daughter minerals and homogenization temperatures up to 467 °C and much higher salinities (up to 55 wt.% NaCl equivalent). Inclusion types 1 and 3 were found to coexist, suggesting either from the trapping of boiling fluids or two distinct immiscible fluids, probably magma-derived. Morales-Ruano et al. (2002) interpreted the fluid history as complex, involving boiling, cooling and mixing of hypersaline magma-derived fluid with surface-derived vapour-rich fluid. Additional information was derived from oxygen isotope systematics in quartz. The narrow range of δ^{18}O values of quartz

(10.8‰ to 12.7‰) was taken as support for fluid mixing. Interestingly, they too the similar δ^{34}S ranges of ore sulphides (−2.3‰ to 6.4‰) and disseminated sulphides in the Moonta Porphyry and interdigitated Doora Schist (−1.5‰ to 4.6‰) to suggest assimilation of crustal sulphur by the granitic magma or ore fluids.

Microscopic investigation during the present study did not reveal the presence of minerals, which could be used as reliable geothermometers; arsenopyrite, for example, was conspicuously found to be absent. Additionally, minerals likely to contain fluid inclusions were also unfortunately found to be extremely scarce (inclusions in sphalerite can only be analysed using an infra-red light source). Indirect constraints on the maximum temperature of ore formation are, however, derived from published experimental work in the ternary system Fe-S-O. The highest temperature that bornite-chalcopyrite-pyrite can coexist in equilibrium with sulphur liquid and vapour, is the lower invariant temperature of 568°C (Roseboom and Kullerud, 1958). The homogenization temperatures of Morales-Ruanao et al. (2002) are, however, at the uppermost range of temperatures for IOCG systems in the Olympic Cu-Au Province.

Genetic model

The location of the Moonta orebodies within shear zones immediately adjacent to the Moonta Porphyry (Figure 20 from Conor *et al.* 2010) suggested to early workers that there was a genetic relationship between the ores and the associated felsic intrusion. We now know that the Moonta Porphyry belongs to an older granite generation (Fanning et al., 2007), inferring that either there is no genetic relationship between the Moonta Porphyry and sulphide ore, or that the Moonta ore pre-dates the assumed 1.6

Ga mineralization event. Geochronological data from ore minerals, or at least other hydrothermal phases associated with ore, would be required to unequivocally constrain the age of mineralization.

Conor *et al.* (2010) have outlined the main ingredients for IOCG mineralization in the Moonta area. These include ductile shear to open upon conduits for hydrothermal fluids, thermal gradients to drive fluid migration and porous host rocks.

Several observations made during the present study suggest that the Moonta-Wallaroo area was affected by multiple mineralization events, or at least that the mineralization event can be sub-divided into successive stages. Illustrative of this is the diversity of pyrite morphologies observed in a number of samples. Even within the same sample (162/53), at least two different varieties are seen (Figure 16). Analogously, the observation of both deformed and less-deformed bornite strongly suggests at least an overprinting (thermal?) event that resulted in sulphide re-equilibration and/or recrystallization. The distinct sub-types of chalcopyrite, although less well understood, may also be evidence for sequential events. Last but not least, the presence of pyrite, pyrrhotite, magnetite and hematite demonstrates that assemblages recognized in the deposit reflect an evolutionally history in fS_2-fO_2 space, tentatively interpreted as a shift towards increasingly oxidized conditions.

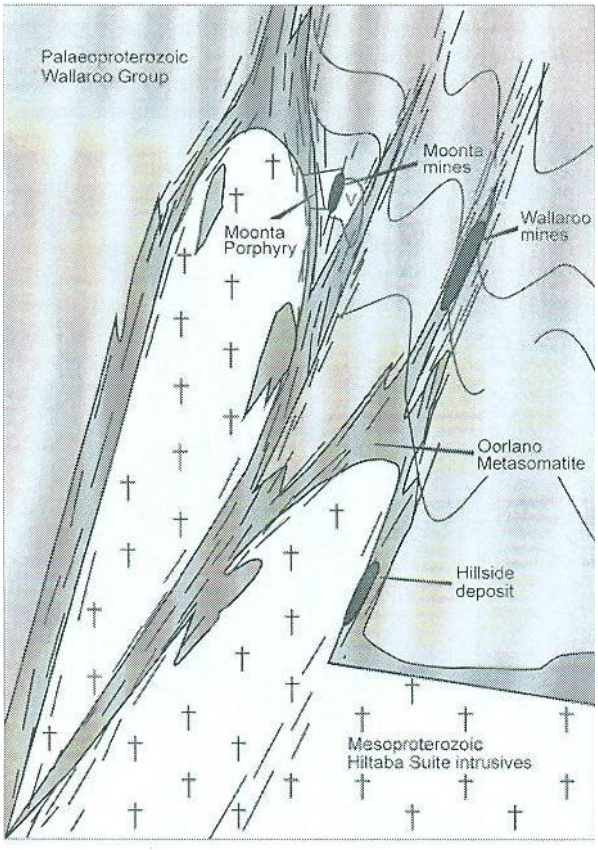

Figure 20*: Schematic diagram illustrating the main ingredients for IOCG-style mineralization in the Moonta area (sourced from Conor et al. 2010)*

Comparison with other IOCG mineralization in the Olympic Cu-Au Province

This study has shown that the Moonta mineralization displays some similarities but also some differences if compared with others in the Olympic Cu-Au Province. The component minerals, dominated by bornite and chalcopyrite, but with lesser pyrite, chalcocite and other Cu-(Fe)-sulphides are clearly similar to other examples. Many of the textures are also highly reminiscent of those seen elsewhere, notably the contradictory replacement of bornite by chalcopyrite and chalcopyrite by bornite, or late Fe-oxide overgrowths on sulphide assemblages. The presence of relatively rare minerals such as cobaltite or ferberite is also consistent with observations elsewhere. So far as it can be judged from samples of massive ore, alteration is also comparable,

notably the recognition of albitization as a relatively early alteration stage.

The abundant pyrrhotite is, however, somewhat unusual. The highly-reduced conditions needed for pyrrhotite stability have not been observed at Olympic Dam, Prominent Hill or other larger sericite-altered IOCG ore systems in South Australia. Pyrrhotite-magnetite assemblages are, however, abundant in deeper, IOCG-related Fe-Cu ore systems, such as Cairn Hill.

The Olympic Dam deposit comprises hematite-quartz breccias, the preferred hosts for economic mineralization (e.g. Reynolds 2001). The OD economic breccia's were thought to have formed as a result of a combination of five processes: hydraulic fracturing; tectonic faulting; chemical corrosion; phreatomagmatic activity; and gravity collapse (Hughes, 1990). The absence of breccias at Moonta is consistent with a somewhat deeper environment than the close-to-surface Olympic Dam system.

The Moonta samples display little similarity with ores from the Hillside deposit and other prospects on the western margin of the Yorke Peninsula. Hillside is characterized by chalcopyrite, with very rare hypogene bornite or chalcocite, and an alteration assemblage dominated by skarn silicates (Ismail et al. 2014).

Implications and future work

The Moonta-Wallaroo area is presently an active exploration area with several companies evaluating a number of prospects across the area. Identified mineralization varies widely in style and composition and display combinations of lithological and structural control. An integrated genetic mineralization model for IOCG-style

mineralization across the area would be an advantage in future exploration. The present study, based around polished sections prepared from precious sample material, will doubtless contribute to this. Future detailed microanalysis of the sample material (e.g., determination of bornite stoichiometry, or trace element fingerprinting of Fe-oxides) may provide additional petrogenetic information beyond the scope of the present project.

CONCLUSIONS

This study has shown that massive copper ores from the Moonta and Wallaroo Mines share a number of similarities with other IOCG systems in the Olympic Cu-Au Province. The component minerals, dominated by bornite and chalcopyrite, but with lesser pyrite, chalcocite and other Cu-(Fe)-sulphides are clearly comparable. Many ore textures are also similar, notably the replacement of bornite by chalcopyrite and chalcopyrite by bornite, or late Fe-oxide overgrowths on sulphide assemblages suggestive of multiple episodes of ore crystallization. Other mineralogical features, such as the abundant pyrrhotite, appear to be a reflection of unusually reduced conditions, probably shifting towards increasingly oxidized conditions at final stages.

Observations do not contradict established models of ore genesis. The Moonta orebodies are the products of IOCG-style mineralization and display strong structural control. Ore-forming fluids were likely derived from Hiltaba Suite intrusives and driven along shear zones.

The present study, based around polished sections prepared from precious sample

material collected more than 50 years ago contribute to a genetic model that takes account of the diversity of mineralization styles, which can assist with ongoing exploration in the Moonta-Wallaroo area.

SPECIAL THANKS

I would like to express my gratitude to Dr. Nigel Cook for all his input, especially within the busiest time of year, Adelaide Microscopy for allowing after-hours access to help me achieve precious images to conclude my study. Finally, I would like to thank Erica Maud McBriar for your past contributions to the research topic, access to your research and a collection of your sample suite.

REFERENCES

Bastrakov, E. N., Skirrow, R. G. ,Davidson, G. J., 2007. Fluids in subeconomic Fe oxide Cu-Au systems of the Olympic Cu-Au-(U) province. *Economic Geology*, 102: 1415-1440

Ciobanu, C. L., Wade, B. P., Cook, N. J., et al., 2013. Uranium-bearing hematite from the Olympic Dam Cu–U–Au deposit, South Australia: A geochemical tracer and reconnaissance Pb–Pb geochronometer. *Precambrian Research*, 238(0): 129-147

Conor, C., 1996. Curnamona, Moonta and Cloncurry: Common Styles of Alteration and Mineralisation linked by the Diamantina Orogen. *South Australia MESA Journal*

Conor, C., Raymond, O., Baker, T., et al., 2010. Alteration and Mineralisation in the Moonta-Wallaroo copper-gold Mining Field Region, Olympic Domain, South Australia. *Hyrothermal Iron Oxide Copper-Gold & Related Deposits: A Global Perspective*, 3

Creaser, R. A. ,Cooper, J. A., 1993. U-Pb geochronology of middle Proterozoic felsic magmatism surrounding the Olympic Dam Cu-U-Au-Ag and Moonta Cu-Au-Ag deposits, South Australia. *Economic Geology*, 88: 186-197

Daly, S., Fanning, C. ,Fairclough, M., 1998. Tectonic Evolution and Exploration potential of the Gawler craton, South Australia. *Journal of Australian Geology and Geophysics*, 17: 145-168

Davidson, G. J. ,Paterson, H., 1993. Oak Dam East: A prodigous, uranium-bearing, massive iron-oxide body on the Stuart Shelf. *Geological Society of South Australia*, 34: 18-19

Ehrig, K., McPhie, J. ,Kamenetsky, V., 2012. Geology and mineralogical zonation of the Olympic Dam Iron Oxide Cu-U-Au-Ag deposit, South Australia. *Special Publication Number 16 - Geology and genesis of major copper deposits,* Society of Economic Geologists, 237-267.

Fanning, C., Reid, A. ,Teale, G., 2007. A geochronological framework for the Gawler Craton, South Australia. *Primary Industries and Resources South Australia, Adelaide*, Bulletin 55

Ferris, G. M., Schwarz, M. P. ,Heithersay, P., 2002. The geological framework, distribution and controls of Fe-oxide and related alteration, and Cu–Au mineralisation in the Gawler Craton, South Australia. Part 1, Geological and tectonic framework. *Hydrothermal iron oxide copper-gold and related deposits: A global perspecitve* 2: 9-31

Forbes, C. J., 2012. Report on production of first version of top of basement solid geology map for the central Yorke Peninsula, Project 3.2/3.3: Yorke Peninsula Project, DET CRC.

Fraser, G., McAvaney, S., Neumann, N., et al., 2010. Discovery of Early Mesoarchean crust in the eastern Gawler Craton, South Australia. *Precambrian Research*, 179: 1-21

Groves, D. I., Bierlein, F. P., Meinert, L. D., et al., 2010. Iron Oxide Copper-Gold (IOCG) Deposits through Earth History: Implications for Origin, Lithospheric Setting, and Distinction from Other Epigenetic Iron Oxide Deposits. *Economic Geology*, 105(3): 641-654

Hampton, S., 1997. A study of the paragenesis and controls of Proterozoic (Cu-Fe-Au-REE) mineralization at the Manxman a1 and Joes Dam South prospects, Mount Woods Inlier, South Australia. *Unpublished Honours Thesis, Australia, Department of Economic Geology, James Cook University of North Queensland*: 146

Hand, M., Reid, A. ,Jagodzinski, R., 2007. Tectonic framework and evolution of the Gawler Craton, South Australia. *Economic Geology*, 102: 1377-1395

Hayward, N. ,Skirrow, R. G., 2010. Geodynamic setting and controls on iron oxide Cu-Au (±U) ore in the Gawler Craton, South Australia. *Hydrothermal iron oxide copper-gold and related deposits: A global perspecitve*, 3(advances in the understanding of IOCG deposits): 105-131

Hughes, F. E., 1990. Geology of mineral deposits of Australian and Papua New Guinea.

Australian Institute of Mining and Metallurgy, 14: 1009-1035

Jack, R. L., 1917. The Geology of the Moonta and Wallaroo Mining District. *S.A. Department of Mines, Geological Survey.*, 6

Kontonikas-Charos, A., 2013. Albitization and REE-U -enrichment in IOCG systems: Inisights from Moonta-Wallaroo, Yorke Peninsula, South Australia.

McBriar, E. M., 1962. Primary Copper Mineralisation at Moonta and Wallaroo, South Australia. *Department of Geology, University of Adelaide*

McPhie, J., Kamenetsky, V. S., Chambefort, I., et al., 2011. Origin of the supergiant Olympic Dam Cu-U-Au-Ag deposit, South Australia: Was a sedimentary basin involved? *Geology*, 39(8): 795-798

Morales Ruano, S., Both, R. A. ,Golding, S. D., 2002. A fluid inclusion and stable isotope study of the Moonta copper–gold deposits, South Australia: evidence for fluid immiscibility in a magmatic hydrothermal system. *Chemical Geology*, 192(3–4): 211-226

Plimer, I., 1980. Moonta-Wallaroo District, Gawler Block, South Australia: A review of the geology, ored deposits and untested potential of EL 544. *South Australian Department of Mines and Energy*: 1129-1200

Reid, A., Hand, M., Jagodzinski, E., et al., 2008. Palaeoproterozoic orogenesis within southeastern Gawler Craton, South Australia. *Australian Journal of Earth Sciences*, 55: 449-471

Reid, A. ,Hand, M., 2012. Mesoarchean to Mesoproterozoic evolution of the southern Gawler Craton, South Australia. *Geological Survey of South Australia*, 35(1): 216-225

Roseboom, E. H. ,Kullerud, G., 1958. The solidus in the system Cu-Fe-S between 400° and 800°C. *Annual Report of Director of Geophysical Lab, Washington.*: 222-227

Skirrow, R. G., Bastrakov, E. N., Davidson, G. J., et al., 2002. The geological framework, distribution and controls of Fe-oxide Cu-Au mineralisation in the Gawler Craton, South Australia. Part II-alteration and mineralisation. in - Porter, T.M. (Ed), 2002 - Hydrothermal Iron Oxide Copper-Gold and Related Deposits: A Global Perspective, . *PGC Publishing, Adelaide*, 2(33-47)

Skirrow, R. G., Bastrakov, E. N., Barovich, K., et al., 2007. Timing of Iron Oxide Cu-Au-(U) Hydrothermal Activity and Nd Isotope Constraints on Metal Sources in the Gawler Craton, South Australia. *Economic Geology*, 102(8): 1441-1470

Sokoloff, V. P., 1951. Geochemical exploration for copper in the Wallaroo mining district, South Australia. *Geochimica et Cosmochimica Acta*, 1(4–6): 284-298

Webb, A. W., 1978. Geochronology of the younger granites of the Gawler Block and its northwest margin. *South Australian Department of Primary Industries and Resources, Adelaide.*: 65

Wurst, A., 1994. Analysis of late stage, Mesoproterozoic, syn- and post-tectonic, magmatic events in the Moonta sub-domain: implications for Cu-Au mineralisation in the "Copper Triangle" of South Australia. 1-78

Zang, W., Raymond, O. L. ,Conor, C. H. H., 2002. Geology of peninsula and Cu-Au mineralization at Moonta and Wallaroo. *Geological Society of South Australia*: 69

Zang, W., Cowley, W. M. ,Fairclough, M., 2006. Maitland Special, South Australia 1:250 000 geological series explanatory notes SI53-12 *Primary Industries and Resources, South Australia*, 1: 62

APPENDIX

Methodologies

The main task around this project was to produce clear, directional images of mineral relationships within the Moonta-Wallaroo mineralization system to further investigate the history of the area. To do this, Microscopic images taken at Adelaide Microscopy were processed and formatted with image grouping software to provide an easily readable, clear table of figures to insert into this manuscript.

Scanning Electron Microscopy (SEM)

SEM imaging was used to look closely at any sort of mineralization characteristics. By looking closely at mineral grain shapes, sizes, contacts and relationships, information gathered through these characteristics all help indicate the past events temperature and pressure on the region. By knowing the past pressure and temperature, we can understand why it is that these minerals are the way they are now and why there is such vast high percentage mineralization in the Moonta-Wallaroo area. All 20 samples were looked at, at Adelaide Microscopy over a vast period of time. To prepare the samples, first small sections of the original sample suite were cut using a small disc saw in the basement of the Mawson laboratories, Adelaide University, then labelled bags containing each individual sample were sent to __ to create polished block samples. Once the samples were finished, they then were sent to Adelaide Microscopy to be carbon coated for use in the Scanning Electron Microscope.

Reflected Light Microscopy

Reflected Light Microscopy was used to locate any features within the mineralization that the SEM couldn't pick up, mostly visual textures were analysed on the reflected Light Nikon Eclipse LV100 POL Petrographic Microscope and only certain samples were analysed. The samples were already prepared from the SEM imaging, carbon coating had to be removed with diamond paste and a polishing block to create clear, impurity free images.(Ehrig et al., 2012)

Additional Figures

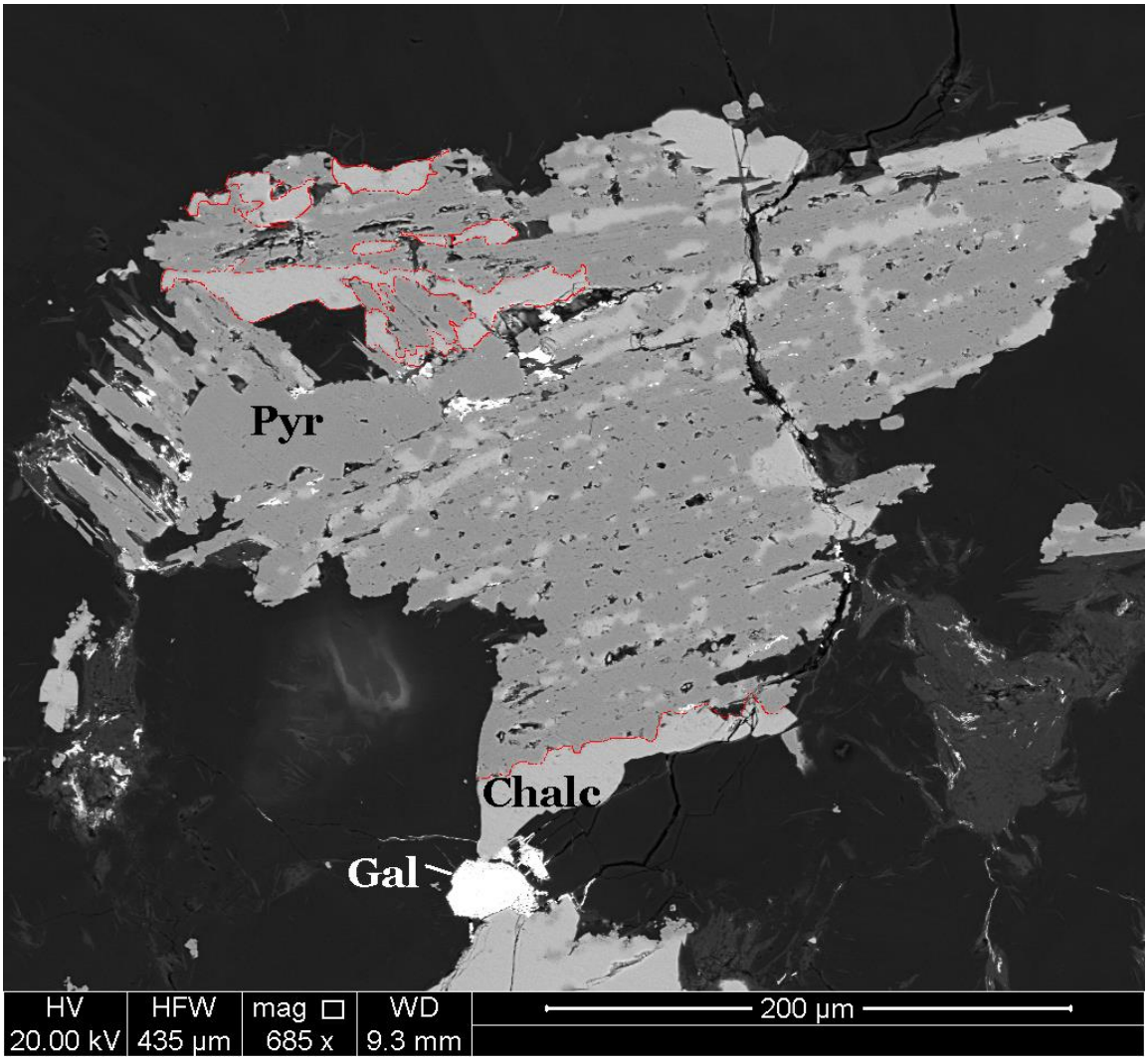

Figure 21: *Sample 162/53 – Sphalerite Sulfide: A grain of Iron rich sulfides, Cu Zonation within the grain. The red line designates cu rich areas, those areas being determined as Chalcopyrite. The Cu Poor areas are pure Fe and S, with ratio of 1:2 favouring Sulfur, hence Pyrite. There are also small grains of Galena in the Sphalerite dominated sample.*

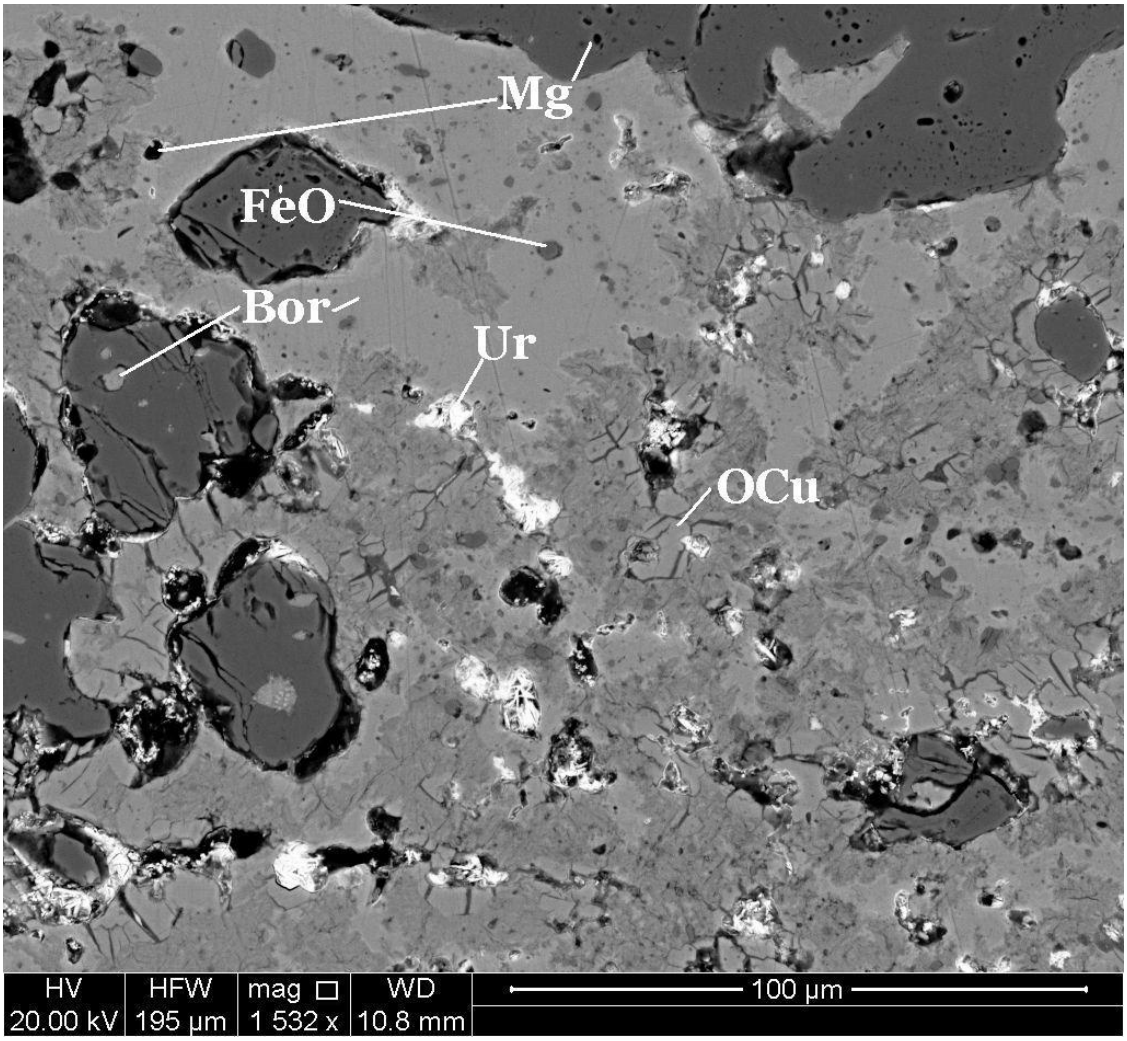

Figure 22: *Sample 162/59 – Bornite Sulfide: Uranium rich grains are within the voids of the bornite dominated groundmass. Hematite grains include inclusions of bornite and magnetite inclusions.*

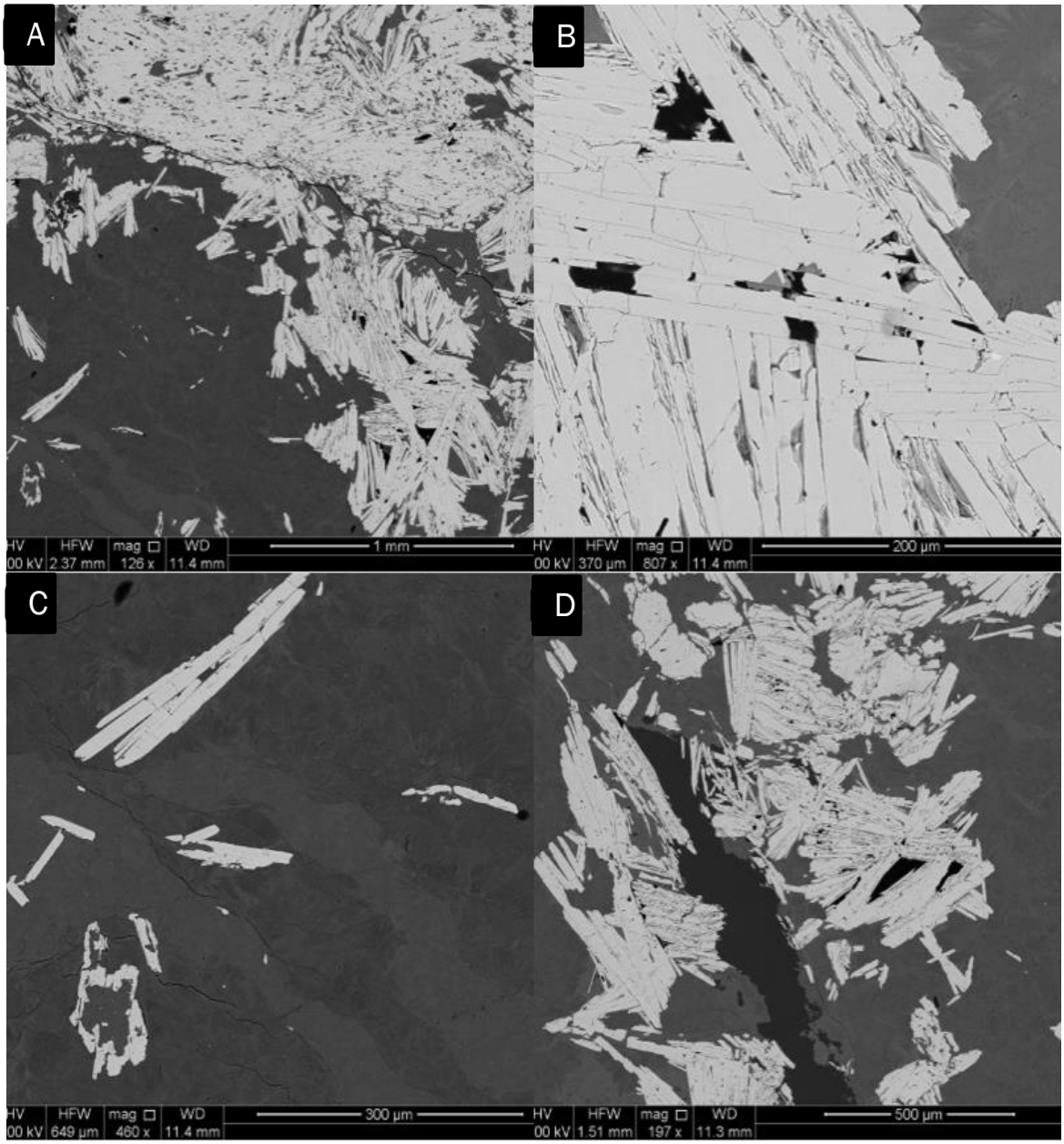

Figure 23: *Sample 162/106 – Moonta Hematite: (a) Iron Oxide Hematite needles are spontaneous and are not in a lamellae form in amongst the aluminosilicate gangue, (b) Some Hematite needles contain inclusions from the aluminosilicate groundmass, (c) Some Hematite needles look like they have been eaten away from the inside, (d) Elongate quartz grains are spread amongst the hematite needles almost separating the gangue material*

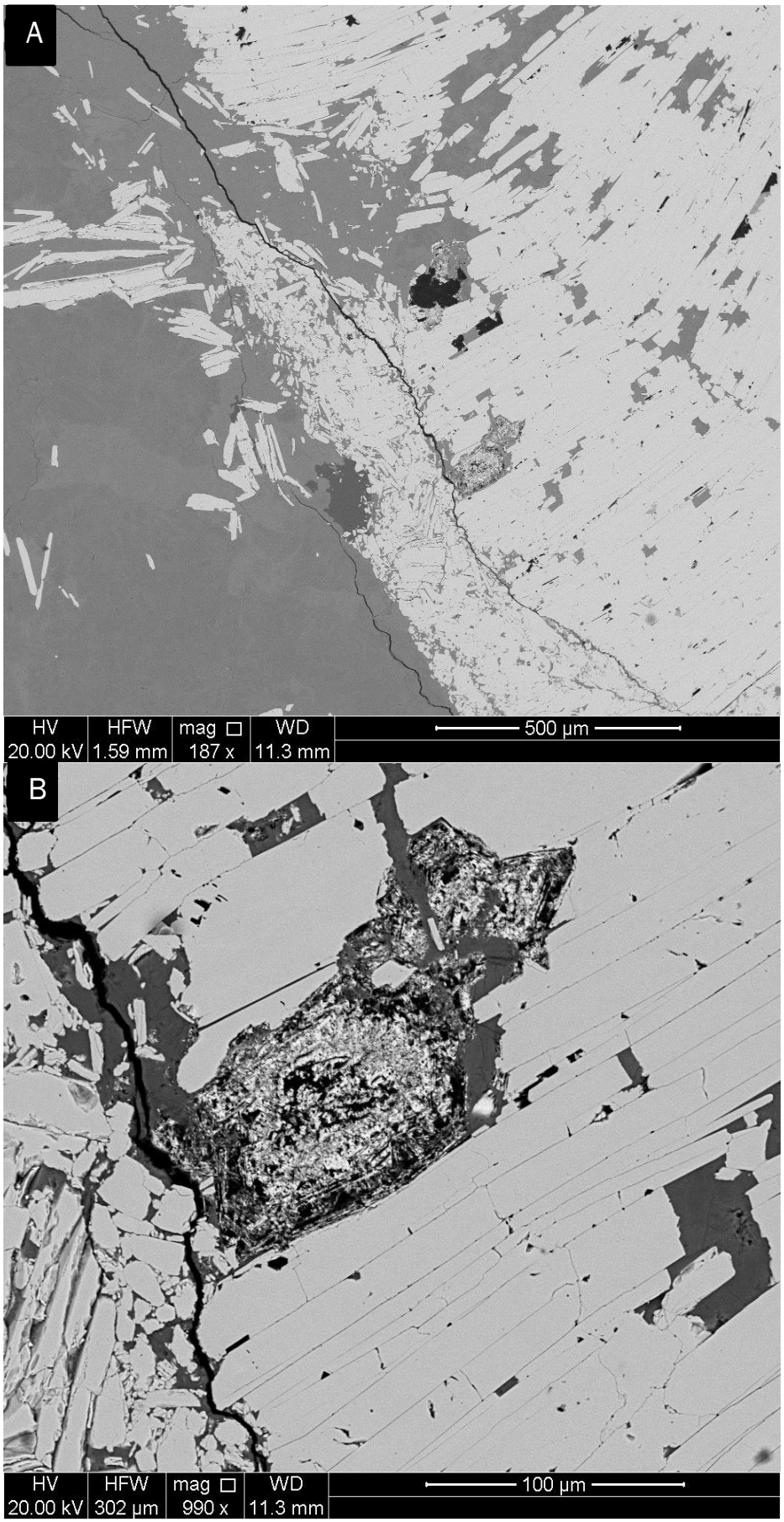

Figure 24: (a) *Sample 162/106 – Moonta Hematite: Big Parallel Fractures run throughout the whole sample, giving distinct growth restrains to the hematite needles, (b) Sample 162/106 – Moonta Hematite: Rare inclusion that is high in Y,Si and O, demonstrates a conchoidal grain distribution.*

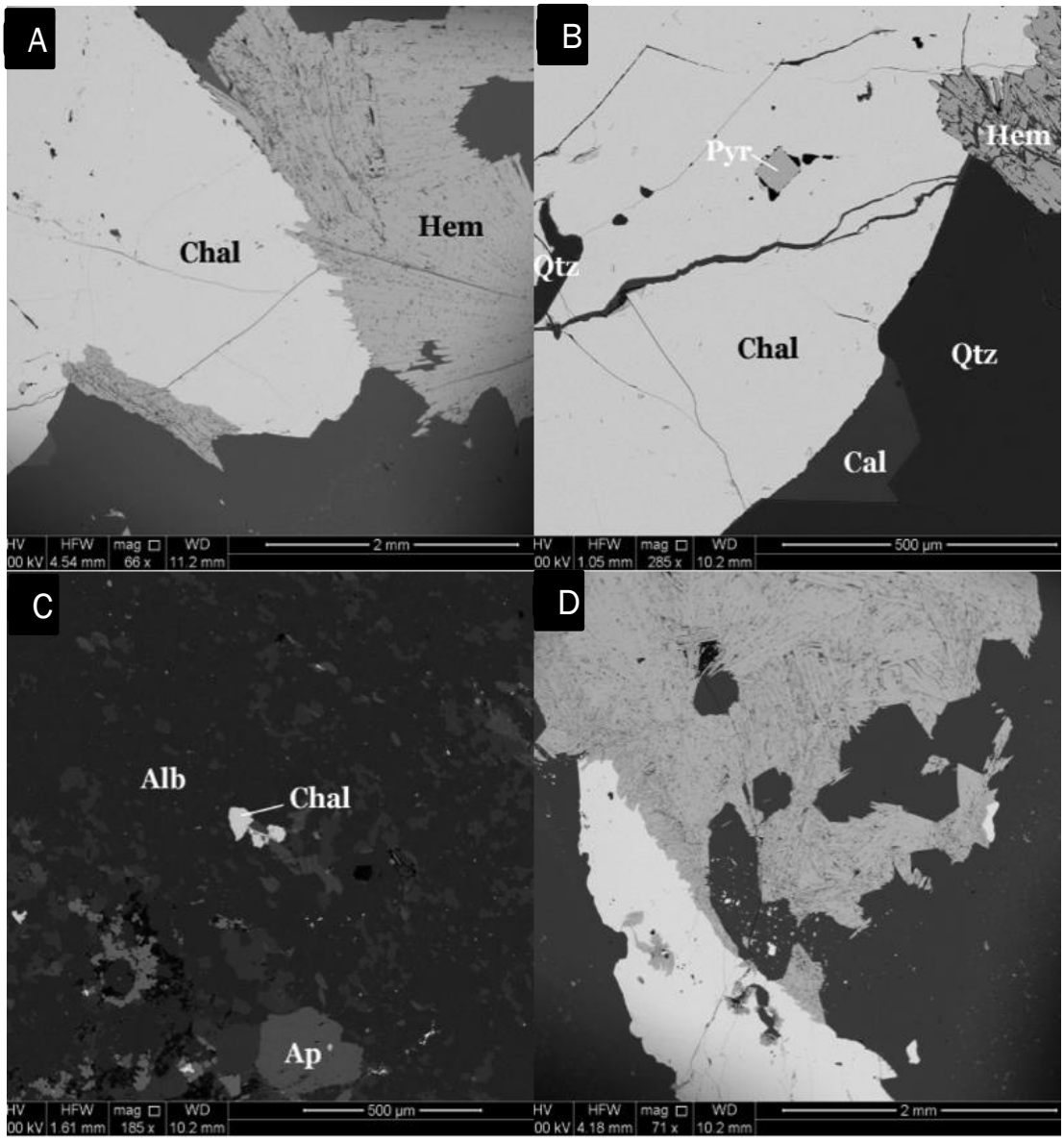

Figure 25: *Sample 162/109 – Moonta Hematite: (a) Chalcopyrite and Hematite border is very sharp, showing no sharing of elements what so ever, (b) Euhedral Pyrite accessory grains within Chalcopyrite, quartz mineral growth through fracture zones, (c) Within the gangue, the majority is made of Albite Plagioclase with grains of apatite (>400um in size) with the odd inclusion of chalcopyrite, (d) Image shows the relationship between hematite and chalcopyrite*

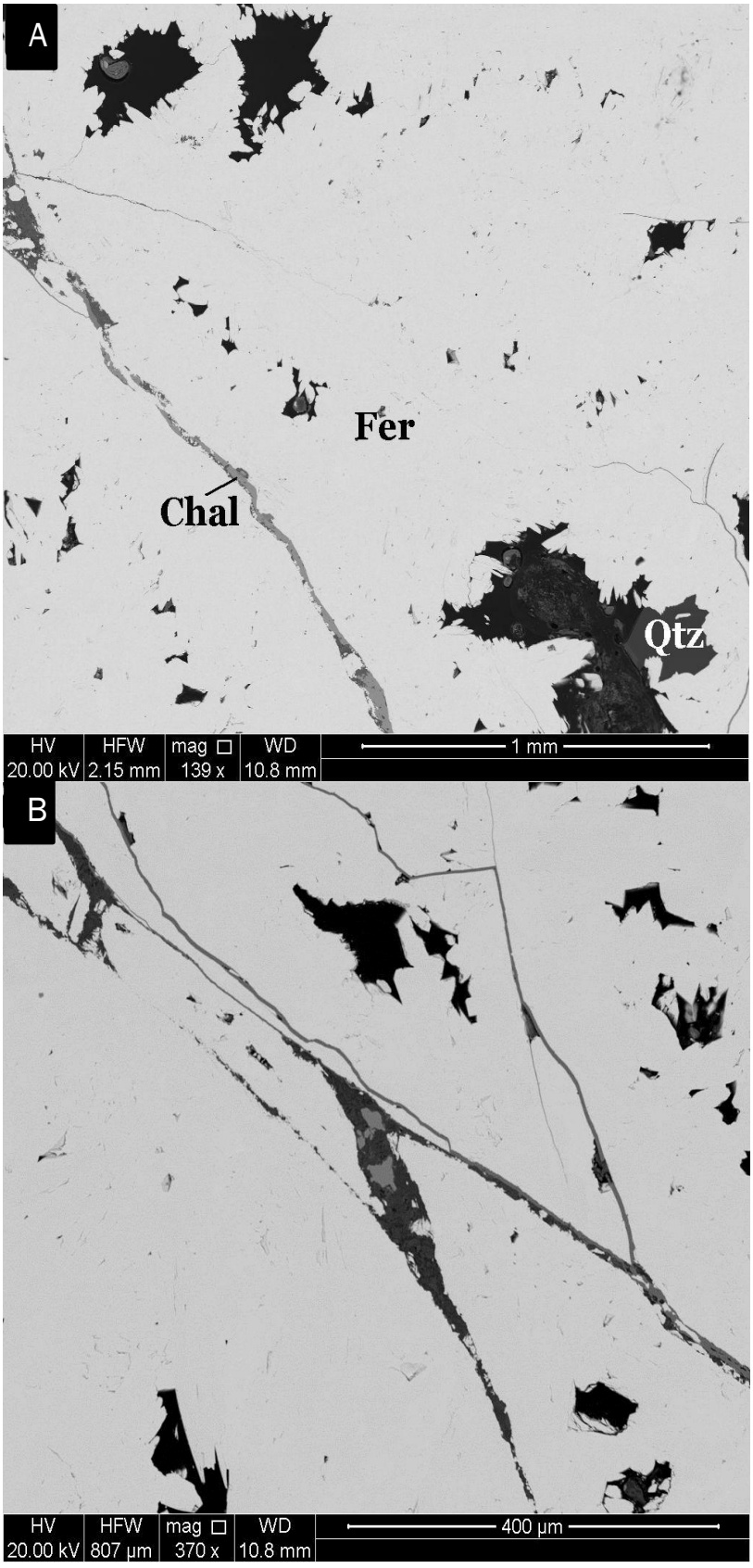

Figure 26: (a) Sample 162/110 – Ferberite: Ferberite grains are somewhat in a needle-type form. Ferberite consists roughly 75% of the sample. Some quartz inclusions are common throughout the voids, long elongate grains of chalcopyrite sulphides are common, (b) Sample 162/110 – Ferberite: The chalcopyrite inhabited elongate grains tend to grow in the fracture plains. Mineralization in the fracture plains also consists of a FeSiO.